Heliyon 10 (2024) e39737

Contents lists available at ScienceDirect

Heliyon

journal homepage: www.cell.com/heliyon

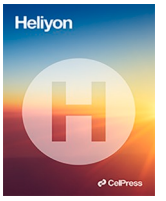

Research article

High temperature pyrolysis of sewage sludge: Synergistic effects of co-pyrolysis with rice straw and composite plastics wastes

Elif Babayiğit [a,b,**], Dilek Alper [a,b], Emine Çokgör [a], Hasan Can Okutan [b,c], Alper Sarıoğlan [b,c,*]

[a] Department of Environmental Engineering, Istanbul Technical University, 34469, Istanbul, Turkey
[b] Synthetic Fuels and Chemicals Technology Center, Istanbul Technical University, 34469, Istanbul, Turkey
[c] Department of Chemical Engineering, Istanbul Technical University, 34469, Istanbul, Turkey

ARTICLE INFO

Keywords:
Sewage sludge
Plastics
Biomass
Pyrolysis
Hydrogen

ABSTRACT

The synergistic effect of co-pyrolysis for the mixtures of sewage sludge (SS), rice straw (RS) and composite plastic wastes (PE&PP) has been investigated with the aim of high gas yields and hydrogen generation. In this context, the applicability of high temperature pyrolysis technology was evaluated at both rotary type batch reactor and rotating screw type continuous reactor operating under the industrially relevant conditions. Gas yields have been improved at increasing the operating temperatures up to 850 °C. The gas yield of 75.06 % with its H_2 portion of 32.35 % has been achieved as the best results for continuous pyrolysis unit at pilot scale. Secondary reactions such as steam de-alkylation, steam cracking, water gas shift and so on were regarded as being responsible for the high gas yields when the primary products of pyrolysis, i.e. condensable vapors, were much exposed to the hot zones inside the reactor. The dehydration of organic components involving the loss of water may supply steam to create a reactive pyrolysis atmosphere. While the pyrolysis of sewage sludge and rice straw favors CO and CO_2 formation due to the high oxygen contents of these feedstocks, more methane and light olefins were produced when the plastics were added to the feedstock blends. This was ascribed to the initially generated radicals from the decomposition of sewage sludge and/or rice straw that might promote the scission reactions of plastics towards volatiles. It was shown that high temperature pyrolysis can be applied to a variety of organic wastes such as rice straw, sewage sludge and waste plastics. Conversion of wastes to hydrogen fosters the circular economy by putting the disposal costs down and creates a new route on renewable hydrogen generation.

1. Introduction

Sewage sludge is a mud-like residue resulting from wastewater treatment. It is a complex mixture of proteins, lipids, polysaccharides, lignocellulosic residues, microplastics, nitrogen- and phosphorous components together with some pathogenics and toxins such as heavy metals, polychlorinated biphenyls etc. Its characteristics vary remarkably depending on the water pollutants, the processes in the treatment plant (physical, physicochemical, biological, etc.) and the quality of the treatment. The current routes for

* Corresponding author. Department of Chemical Engineering, Istanbul Technical University, 34469, Istanbul, Turkey.
** Corresponding author. Department of Environmental Engineering, Istanbul Technical University, 34469, Istanbul, Turkey.
E-mail address: asarioglan@itu.edu.tr (A. Sarıoğlan).

https://doi.org/10.1016/j.heliyon.2024.e39737
Received 8 July 2024; Received in revised form 16 October 2024; Accepted 22 October 2024
Available online 23 October 2024

sludge management were landfill, sea disposal, incineration and agriculture recycling. Its landfilling is problematic due to the pollutant content of the sewage sludge such as volatile organics, heavy metals, micro-plastics and pathogens and this route will be phased out in the near future. Its dumping at sea is an approach taken with reservation globally and this route has already been banned in many countries e.g. in England and Wales in 1998. The third route, incineration is the most expensive route with a significant carbon burden on atmosphere. Although the Sewage Sludge Directive (86/278/EEC) regulates the use of sewage sludge in agriculture by the limits of heavy metals (Cd, Cu, Hg, Ni, Pb and Zn), most of EU countries have started bringing stricter regulations with a lower limit of heavy metals than given in EU Directive [1]. Furthermore, crops fertilized with sludge are not counted suitable for "eco-labeling". To all these objections, the sludge contains valuable organic matter and nutrients such as nitrogen, potassium and phosphor components. Therefore, a cost-effective management of sludge gains importance not only for its environmentally friendly disposal but also in terms of circular economy from waste to sustainable fuels and chemicals [2–4]. Thermochemical conversion technologies such as pyrolysis and gasification are considered promising alternatives to incineration. They have the merits of higher efficiency, greater volume reduction, more added value with a product variety, immobilizing heavy metals and process intensification [5,6]. Pyrolysis does not burn waste by adding air or oxygen and avoids the release of any harmful waste gas. CO_2 capture from the pyrolysis or gasification is less costly than from the flue gas of an incineration plant as well. It helps the neutralization of pathogens during the thermochemical conversion. As a self-sustainable thermochemical conversion route for organic wastes such as plastics, it responses to the decentralized green, renewable hydrogen production for the mobility applications [7,8].

Pyrolysis of the sewage sludge or any other feedstock such as agricultural waste, wood, plastic, and food waste can be briefly defined as its thermal decomposition to syngas, oil and char in the absence of oxygen. Syngas is mainly composed of CO, CO_2, H_2 and CH_4 while oil has a content of phenols, ketones, amines, aliphatic hydrocarbon and aldehydes. These gaseous and liquid pyrolysis products may find use as the raw material for the production of synthetic fuels and chemicals or can be further processed by gasification [9,10]. The other output of pyrolysis, char has high surface area, porosity and cation exchange capacity and holds a great potential for various applications of soil remediation, carbon sequestration, and the removal of hazardous organic compounds and heavy metal cations [11]. Thermochemical conversion might also help the immobilization of heavy metals in char and reduce their bioavailability by forming non-hazardous and chemically stable fractions of these metals [5]. However, there are challenges associated with the pyrolysis of sewage sludge that need to be addressed. One major limitation is the relatively high moisture and ash content of sewage sludge, which results in high-energy consumption during pyrolysis [4]. In order to improve the quality and the product yield of the sewage sludge pyrolysis, strategies such as co-pyrolysis of sewage sludge with other solid wastes and biomass have been proposed [3,4,12–14]. However, synergetic effects in co-pyrolysis depend on operating conditions such as reactor type, heating rate, temperature, contact time, feedstock type and mixture ratios. For example, there is well packing of feedstock in fixed bed reactors but slight interactions of the dispersed particles exist in fluidized bed reactor. Besides, co-pyrolysis occurs in a wide range of temperature in fixed bed due to the slow heating rates whereas high heating rates of fluidized bed reactors shorten the lag time for devolatilization [15].

The COVID-19 pandemic has led to a substantial increase in plastic waste globally, alongside the production of 450 million tons of plastics annually [16,17]. In regarding their potential in circular economy, polypropylene (PP) and polyethylene (PE) are the most common plastics in the content of the municipal solid waste. The high calorific value, H/C ratio, volatility and low ash content of plastics may offset the disadvantages of sludge pyrolysis [18,19]. Co-pyrolysis of sewage sludge and plastics may improve the energy efficiency of the whole process by facilitating the release of volatile matter and lowering the activation energy [20]. Besides, their co-pyrolysis may enhance the syngas yield together with the improved oil and char quality. Altered surface functional groups of char, the reduction of oxygenated compounds and water content of oily product all may come from their synergistic effect [10,20–22]. A decrease in the oxygenated compounds of pyrolysis oil may solve the bio-oil instability, otherwise that can lead to viscosity increase due to the polymerization reactions ending up with deteriorated fuel performance [23].

Biomass is another sustainable feedstock for the co-pyrolysis of sewage sludge due to its high volatile and low ash content [24,25]. Co-pyrolysis of sewage sludge with biomass may be a feasible strategy to resolve the problems such as poor energy efficiency and product quality of the pyrolysis of sewage sludge alone [9,26]. Adding biomass to sewage sludge in an appropriate proportion may homogenize the final mix with predictable mechanical and physicochemical characteristics [23]. Up to date, most of the research has been focused on the co-pyrolysis of sewage sludge either with lignocellulosic biomass or plastics to enhance the pyrolysis oil and char yield but not for the gas products. To the best of our knowledge, hydrogen production via high temperature pyrolysis with ternary mixtures of sewage sludge, biomass and plastic wastes has not been reported yet. Moreover, it is crucial to optimize the proportions of sewage sludge, biomass and plastics wastes in a ternary mixture in order to control the thermochemical conversion for rotary type batch reactor at bench scale. The aim of this study is to investigate the optimum proportion of sewage sludge, rice straw and polyethylene/polypropylene plastics and ultimately to achieve the maximum hydrogen and char yields from their ternary mixtures via high temperature pyrolysis at 850 °C. In this context, the hypothesis of this research is to exhibit the applicability of high temperature pyrolysis technology as a distributed approach in converting solid organic wastes into carbon-negative hydrogen in response to the need on circular economy solutions.

2. Material & methods

2.1. Materials and preparation

The dried and granulated municipal sewage sludge (SS) with irregular shapes and size with an average of 2–4 mm was supplied from a municipal wastewater treatment plant in Turkey. Waste composite labels in polyethylene (PE) and polypropylene (PP) origin were supplied from a domestic label producer. Rice straw (RS) pellets in the dimensions of 2–3 cm length and of 3–4 mm diameter were

provided from Ipsala, Tekirdag in Turkey. For material characterizations, all samples have been grinded and sieved below 0.25 mm. For the pyrolysis tests, composite PE and polypropylene PP labels have been shaped into cylindrical pellets of 5 mm in length and of 4 mm in diameter. Sewage sludge and rice straw have been used as in their supplied granular and pelleted forms, respectively.

SS, PE, PP and RS were used individually or as mixtures in the experiments. For clarity of designation, in double mixes, the blending ratios of sewage sludge to the plastics or biomass were set either as 1:1 or 3:1. In this regard, SSPE, SSPP or SSRS designations stand for the blending ratios of 1:1 on weight basis. Similarly, SS3PP1, SS3PE1 or SS3RS1 designate the blending ratios of 3:1. Triple mixes such as SSPPRS will represent the blending ratios of 2:1:1 for a sewage sludge to PP and to RS as given in Table 1.

2.2. Feedstock and product characterizations

Proximate analysis was performed for the moisture, volatile matter, fixed carbon and ash contents of the feedstock according to ASTM D7582 standard on LECO TGA 701 instrument. Elementar Vario Macro instrument was used for the ultimate analysis of the carbon, hydrogen and nitrogen content according to ASTM D5373. Oxygen content has been calculated from the elementary balance. The higher heating value has been determined according to ASTM D4809 by using LECO AC-600 instrument. Three measurements have been recorded on each sample and the mean value has been considered for reporting in the Tables.

The syngas composition was determined by using a Micro GC (INFICON, Switzerland) equipped with a flame ionization detector (FID) and a thermal conductivity detector (TCD). Determinations were made of H_2, O_2, N_2, CH_4, CO, CO_2, C_2H_4, C_2H_6, C_3H_6, C_3H_8, C_3H_4, C_4H_{10}, C_4H_8, and C_5H_{12}. Hydrocarbon and permanent gases analysis were performed on FID and TCD, respectively and with helium ($\geq$99.99 % in purity and supplied from AirLiquide) as the carrier gas. The gas calorific value has been calculated from the gas composition in accordance with ISO 6976. For the calculations, the calorific values of H_2, CH_4, CO, C_2H_4, C_2H_6, C_3H_6, C_3H_8, C_4H_{10}, C_4H_8, and C_5H_{12} gases were taken as 12.75, 39.72, 12.63, 63.41, 70.29, 93.58, 101.24, 125.09, 133.12 and 147.17 MJ/m^3, respectively [27].

The surface functional groups of biochar samples were evaluated by the Fourier transform infrared spectroscopy (FT/IR-4700, Jasco) at room temperature in the spectral range of 400–4000 cm^{-1} at a resolution of 4 cm^{-1}. Prior to sample measurements, background data were gathered and subtracted in order to prevent any measurement deviations by the noisy from the instrument. The chemical composition of the biochar samples was determined by the X-Ray Fluorescence spectroscopy (XRF, S8 TIGER Series 2, Bruker). For ash composition measurement, the ash of feedstocks were prepared thermally in a muffle furnace at 600 °C for 2 h.

Gas chromatography-mass spectrometer (7890A series GC/5975C series MS, Agilent Technologies, USA) was applied to determine the chemical composition of the bio-oil products. Approximately 40 mg of bio-oils were dissolved in 1 mL of acetone (analytical grade of $\geq$99.8 % and supplied from Merck), and the diluted samples were dehydrated with 200 mg of magnesium sulfate heptahydrate (analytical grade of >99.5 % and supplied from Ferak Berlin) and filtered through a 0.45 μm PTFE syringe -driven filter (supplied from ISOLAB) before injection. The GC separation was carried out using an HP-INNO Wax capillary column (30 m × 0.25 mm × 0.25 μm), and Helium ($\geq$99.99 % in purity and supplied from AirLiquide) was used as the carrier gas. A sample injection volume was 1 μL and the solvent delay was set at 2.8 min. The GC oven temperature was ramped from 50 °C to 230 °C (50 °C for 2 min, 10 °C/min to 90 °C, 4 °C/min to 120 °C, 8 °C/min to 230 °C, and 230 °C for 10 min) and the mass selective detector in electron impact ionization mode. Identification of peaks was based on computer matching of mass spectra on Wiley MS library and literature data.

2.3. Thermogravimetric analysis

Thermogravimetric analysis (TGA) of each feedstock (SS, PE, PP, RS) and their double and ternary mixtures have been carried out under pyrolysis conditions by using TGA 55 Model TA Instruments. Measurement conditions were given in Table 2. The derivative weight loss (DTG) profiles for all samples were driven from their TGA measurement data and further evaluated.

Table 1
Designations of samples used in the experiments.

Designation	Composition (%)			
	Sewage Sludge (SS)	Polyethylene (PE)	Polypropylene (PP)	Rice Straw (RS)
SS	100	0	0	0
PE	0	100	0	0
PP	0	0	100	0
RS	0	0	0	100
SSPE	50	50	0	0
SS3PE1	75	25	0	0
SSPP	50	0	50	0
SS3PP1	75	0	25	0
SSPEPP	50	25	25	0
SSRS	50	0	0	50
SS3RS1	75	0	0	25
SSPERS	50	25	0	25
SSPPRS	50	0	25	25

Table 2
TGA conditions for the pyrolysis of the samples.

Initial weight	N_2 flow rate	Fine powder sample size	Heating rate	Initial-final temperature
~35 mg	40 ml/min	<250 μm	10 °C/min	25–850 °C

2.4. Pyrolysis tests in the rotary type batch pyrolysis unit

A series of experiments were carried out in the batch pyrolysis unit at the bench scale with 1–3 kg feedstock per batch. The photo and the block diagram of the batch pyrolysis unit were shown in Fig. 1(a) and (b), respectively. The content of the cylindrical flanged tube reactor is continuously mixed with blades constructed on a rotating shaft. The rotational speed of the shaft is adjusted remotely with a control program. A purge line on one side of the reactor allows the pyrolysis reaction occur under inert or reactive gas atmospheres. The temperature of the reactor is controlled by thermocouples from the inside of the oven but on the outside surface of the reactor. The system has a wax/oil trap, a cooling column, and an open spray type scrubber. Pyrolysis gas, when it was stripped from its oily and wax compounds, was sampled by the syngas analyzer (MRU SWG 200). All gas products were combusted at flare and combustion gases were vented to the atmosphere. At the end of tests, the reactor is cooled down to ambient temperature under nitrogen gas atmosphere (≥99.995 % in purity and supplied from Linde). Then, solid carbonaceous residue (char) is taken from the reactor and weighed for mass balance calculations. Wax, oily and aqueous products are collected from the traps and the containers under the cooler and scrubber columns, respectively. Gas yield is calculated by subtracting the collected char and wax/liquid products from the weight of the pyrolyzed feedstock for that batch.

For each batch of experiments, 0.5 kg of sewage sludge or its double or ternary mixtures with plastics and biomass was used. The rotational speed of the reactor was set to 5 Hz corresponding to 3 rpm for all experiments. All pyrolysis tests have been carried out at three different temperatures of 750 °C, 800 °C and 850 °C in order to investigate the high temperature pyrolysis of these composite wastes. Vapor residence time was changed by the flow rate of nitrogen carrier gas. Three different nitrogen flow rates of 0.5 l/min, 1.0 l/min, and 1.5 l/min have been used to examine the effect of residence time on product distribution.

2.5. Pyrolysis tests in the screw type continuous pyrolysis unit

Pilot scale pyrolysis unit was the an indirectly heated screw conveyor type system with a feeding capacity up to 10 kg/h which was being operated in continuous mode. This system has been used to perform the experiments in conditions closer to the industrial environment to complement the bench scale tests. The pilot scale pyrolysis reactor has a diameter of 30 cm and a length of 230 cm. The photo and the block diagram of the continuous pyrolysis unit were shown in Fig. 2(a) and (b), respectively. The system is composed of a feeding bunker, pyrolysis reactor, char collection tank, electrically heated cyclone as for thermal cracker, an integrated heat

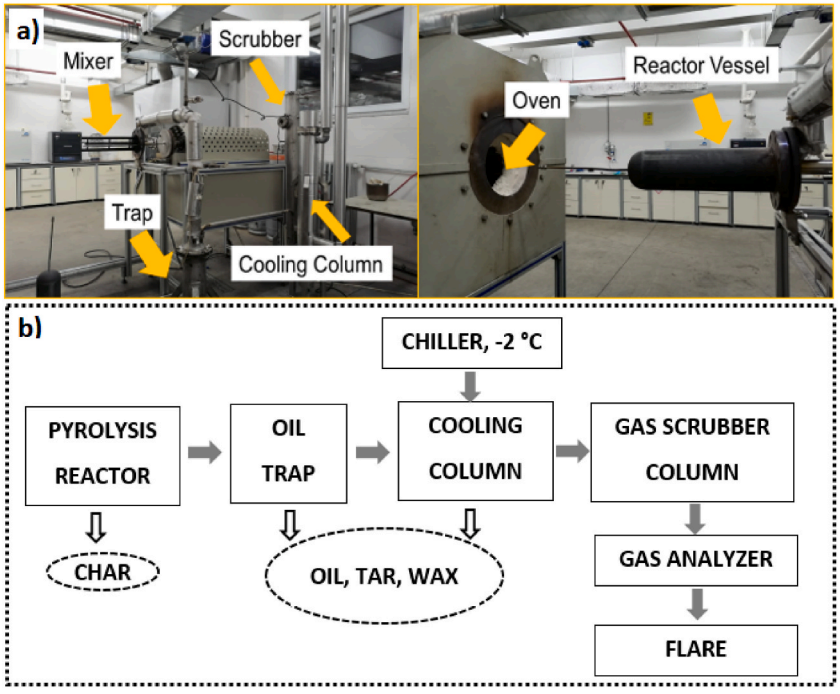

Fig. 1. (a) The photo of the batch pyrolysis unit, (b) Block diagram of the batch pyrolysis unit.

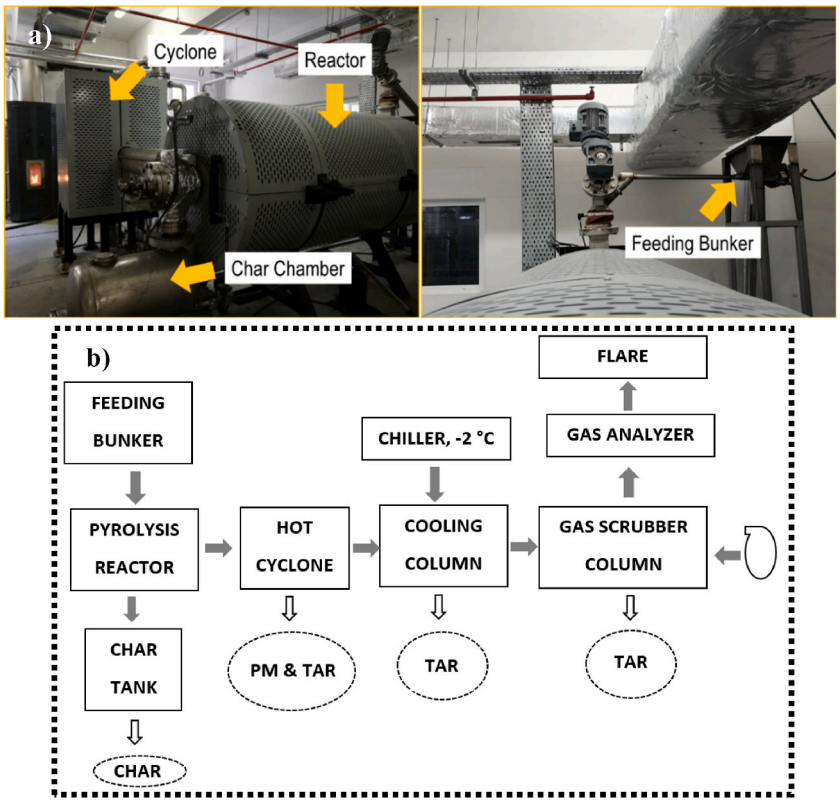

Fig. 2. (a) The photo of the continuous pyrolysis unit, (b) Block diagram of the continuous pyrolysis unit.

exchanger, open spray scrubber and an industrial chiller for gas cooling and tar removal and finally a flare for safely venting the off gases. An online syngas analyzer, (MRU SWG 200) was used for monitoring the gas release and the composition. All input/output variables have been remotely controlled and monitored via a Programmable Logic Controller-PLC (Scada) system.

Once the pyrolysis system reached the desired temperature of 850 °C, the feedstock was loaded into the bunker and fed into the reactor at a controlled feed rate of 2.5 kg per hour using an endless screw rotating at 20 Hz, a value determined through calibration tests. For inertness of the operation, 2 L/min N_2 flow was used as well. The char was collected in the chamber being located downstream of the pyrolysis reactor, while the liquid vapors and gaseous products keeps flowing over electrically heated lines to hot cyclone kept at 400 °C. Particulates and condensable tar compounds at 400 °C were separated from the bottom of hot cyclone. Then pyrolysis gas was cooled down by shell and tube-type heat exchanger and open spray column installed in the downstream of hot cyclone. The pyrolytic oil was condensed at both of the units and relatively clean pyrolysis gas was flared before venting. A split stream in front of the flare line was sucked by the online gas analyzer (MRU SWG 200) for the analysis of O_2, CO_2, CO, H_2, and CH_4 components present.

2.6. The basis of calculations

The effective hydrogen-to-carbon atomic ratio (H/C_{eff}) has been calculated by

$$H/C_{eff} = \frac{mol\ of\ H - (2\ x\ mol\ of\ oxygen) - (3xmol\ of\ nitrogen) - (2xmol\ of\ sulfur)}{mol\ of\ C} \quad (1)$$

where N, S, H, O and C represent their number of atoms in the feedstock.

The char yield was calculated as the ratio of the amount of collected char to the total amount of the feedstock fed throughout the experiment as given in the following equation:

$$Char\ yield\ (wt.\%) = \frac{\text{the amount of collected char}}{\text{the total amount of the feedstock fed}} \times 100 \quad (2)$$

The heating value of the pyrolysis gas has been calculated in accordance with ISO 6976 based on the gas composition analysis.

The theoretically expected char yields for sewage sludge (SS) mixtures with polyethylene (PE), polypropylene (PP) and rice straw (RS) have been calculates as:

$$Y_{cal} = X \times Y_{WS} + (100 - X) \times Y_{SS} \quad (3)$$

where Y_{cal} is the theoretically expected char yield.

X is the weight percentage of RS, PE or PP in the mixture; and.

Y_{SS} and Y_X (Y_{WS}, Y_{PE} Y_{PP}) are the individual char yields, respectively.

3. Results and discussion

3.1. Feedstock characterization

Sewage sludge has a complex mixture containing proteins, lipids, polysaccharides, lignocellulosic residues, micro plastics, nitrogen- and phosphorous components together with some pathogenics and toxins such as heavy metals, polychlorinated biphenyls, etc. By omitting its high ash content, biogenic residues and micro plastics can be considered as its major constituents. The contribution of these two major components and interactions each other in high temperature pyrolysis was intended for clarification. For this reason, rice straw as biogenic waste has been used without blending or rice straw and PE/PP plastics have been used in different blends with sewage sludge. These feedstocks in different blends have been exposed to high temperature pyrolysis. The proximate and ultimate analysis with the calorific values of each feedstock were given in Table 3. As seen in Table 3, the fixed carbon content of sewage sludge and rice straw were calculated as 6.7 % and 11.6 %, while there is almost no fixed carbon in the content of waste plastics. Based on this, the fixed carbon content of resultant chars would be high upon the amount of sewage sludge and rice straw in the blends. As reported by Zhao et al. [28], fixed carbon content of char is a measure of recalcitrance, resistance to abiotic and/or biotic degradation that improves its atmospheric carbon sequestration in soil. Therefore, the use of rice straw with the highest fixed carbon content among all would be advantageous.

The volatile matter of each feedstock was the indicative of the pyrolysable fraction. Regarding this, plastics with nearly 100 % volatile matter would have much higher oil and gas yields compared to sewage sludge and rice straw. In the other side, the organic nature of the volatile matter is decisive on the degradation mechanism and hence the efficiency of the decomposition. Moreover, synergistic or adverse effects would exist for the co-pyrolysis of the feedstock with different volatile matters in nature, i.e. the formation of radicals in the earlier degradation period of lignocellulose may improve the depolymerization rate of the plastics [29].

Regarding the ash content, both sewage sludge and rice straw have high ash contents of 39.4 % and 17.9 %, respectively while the plastics are almost free from ash. High ash content leads to an increase in the amount of char at the expense of pyrolysis oil and gas yields. The possible catalytic effects of ash, particularly alkali metals, may promote the quality of the pyrolysis products as well.

In terms of elemental composition, sewage sludge had a carbon and oxygen contents of 29.5 % and 20.5 % that were the amounts in between those of rice straw and plastics. Plastic wastes of PE and PP have much higher carbon contents due to their molecular nature. Regarding the nitrogen content, sewage sludge had the highest nitrogen content of 5.6 % that might cause its release as ammonia in syngas and formation of nitrogen tar compounds such as indole and methyl indole in liquid product. In the co-pyrolysis, more nitrogen might be retained in the sludge char with the addition of biomass or waste plastics as reported by Shen et al. [18] and Zhang et al. [30] and can be expected in this study as well.

It is noteworthy that plastics have hydrogen contents twice as high compared to sewage sludge and rice straw. Since the H/C ratio effects on the aromatic carbon efficiency and coke formation, these values have been calculated and interpreted accordingly. Atomic H/C of all feedstock were nearly the same at around 1.8 and 1.9. On the other hand, the use of effective hydrogen to carbon ratio in accordance with Equation (1) has been assessed in terms of the bio-oil upgradability since the relation between the feedstock and ultimate oil quality relies on the effective H/C ratio. As mentioned by Ahmed et al. [31], the pyrolysis oil with H/C_{eff} values beyond 1.0 meets the composition requirements for its upgrading to fuels. Sewage sludge and rice straw have appeared to be in hydrogen

Table 3
The chemical characterization results of sewage sludge, polyethylene and polypropylene wastes and rice straw.

	Sewage sludge (SS)	Polyethylene (PE)	Polypropylene (PP)	Rice straw (RS)
PROXIMATE ANALYSIS (wt. %)				
Original Basis				
Moisture	3.2	0.2	0.2	9.9
Volatile matter (VM)	50.8	99.2	98.4	60.6
Ash	39.4	0.6	1.3	17.9
Fixed carbon (FC)	6.7	0.01	0.1	11.6
ULTIMATE ANALYSIS (dry basis, wt. %)				
Carbon (C)	29.5	81.0	78.1	35.9
Hydrogen (H)	4.5	13.0	12.0	5.5
Nitrogen (N)	5.6	0.05	0.11	1.2
Sulfur (S)	0.6	0.3	0.25	0.2
Oxygen (O)[a]	20.5	5.2	8.3	39.3
O/C	0.52	0.05	0.08	0.82
H/C	1.82	1.93	1.84	1.83
H/C_{eff}	0.27	1.83	1.67	0.10
HEATING VALUES (MJ/kg, dry basis)				
Heating value	13.0	43.2	39.9	13.8

[a] %O = %(100 – (%C + %H + %N + %S + %Ash)).

deficiency as noticed from their calculated $H/C_{eff.}$ ratios of 0.27 and 0.10, respectively. However, $H/C_{eff.}$ ratios of PE and PP have been calculated as 1.7–1.8, which were due to the deficiency of oxygen, nitrogen and sulfur in the content plastics. As claimed by Hu et al. [32], the ring size of the aromatic compounds in pyrolysis oil may change with the H/C ratio of the feedstock where the lowest H/C content favors the smaller ring sized aromatics. Finally, hydrogen-donating role of plastics that changes the pyrolysis liquid product characteristic was generally agreed on [33].

O/C ratios of the feedstock were changing in between 0.05 and 0.82 from plastics to biomass. The shortcoming of high O/C ratio was the production of bio-oil with high oxygen content that was easily oligomerized to form "gummy" solid with a short shelf life. Besides, the presence of organic acids makes the bio-oil highly corrosive. However, the facilitated depolymerization of polyolefins in the presence of biomass oxygenates was claimed by several authors [29,33]. More aromatics formation can be expected through the reaction of furanic compounds with light olefins through the Diels-Alder and subsequent dehydration reactions [31,34]. Therefore, co-pyrolysis of lignocellulosic residues with plastics might be helpful in getting more upgradable liquid products.

Lastly, sewage sludge and rice straw have calorific values of 13.03 MJ/kg and 13.80 MJ/kg, respectively that is quite less compared to plastics of around 40 MJ/kg. The higher C and H contents of plastics were well reflected by their high calorific values. Overall, apparently the pyrolysis behavior of the feedstock depends on both its chemical characteristics and pyrolysis conditions. Therefore, the feedstock characterization results will be further elaborated together with the pyrolysis test results in the following sections.

3.2. Thermogravimetric analysis

3.2.1. Thermogravimetric analysis of SS, PE, PP, and RS as individual

Thermal gravimetric analysis (TGA) of each feedstock alone, namely sewage sludge, waste polypropylene, waste polyethylene and rice straw, have been carried out under the conditions given in Table 2. The measured TGA plots were given in Fig. 3a. The first derivative of the weight loss (DTG) has been calculated and plotted in Fig. 3(b) as well.

Sewage sludge (SS) is a quite complex mixture containing low stability organic compounds, hemicellulose, cellulose, lignin, microplastics, bacteria and inorganics in a diverse and random distribution. Therefore, its thermal degradation profile has expanded across a broad temperature range spanning from 25 °C to 850 °C. The pyrolysis process of SS can be divided into three stages, with the first stage (25–140 °C) primarily involving the dehydration of organic components through the loss of free and chemically bonded water, along with the decomposition of volatile organic compounds. In this stage, the weight loss was recorded as of 6.7 % for SS. In the other side, the removal of moisture from RS occurs in the first stage from 30 to 110 °C, whereas there was no significant weight loss for all plastic wastes until the active pyrolysis stage has started. This was reasonable based on their proximate analysis results.

The second stage pyrolysis of SS and RS starts at 140 °C, where the main thermal decomposition of reactive organics occurs [35,36]. In the range of 140 and 360 °C, the observed weight loss can be ascribed to the thermal decomposition of the organic components such as lipids, proteins, polysaccharides and also of the cellulosic constituents of biogenic wastes. From Fig. 3(a), the weight losses of SS and RS at Stage 2 were observed as 50.0 wt% and 60.0 wt%, respectively. From their DTG profiles, thermal decomposition of SS has started earlier than RS. This proves its heterogeneous nature since SS contains other volatile components in addition to cellulose and hemicellulose. Although two of the feedstocks, SS and RS, have shown a similar DTG profile in this range, RS appeared to be thermally decomposed significantly faster than SS. On the other hand, weight loss in this region was not significant for the plastic wastes, namely started from 280 °C and peaked close to 396 °C for PP and to 456 °C for PE. It was obvious that sewage sludge and rice straw had been decomposed to a large extent before the plastic wastes started to decompose. As mentioned in the feedstock characterization section, the formation of radicals in the earlier degradation period of lignocellulose might improve the depolymerization rate of plastics. As shown in Fig. 3(b), the thermal degradation of polyethylene plastic wastes has been started at about 250 °C and the rates of their

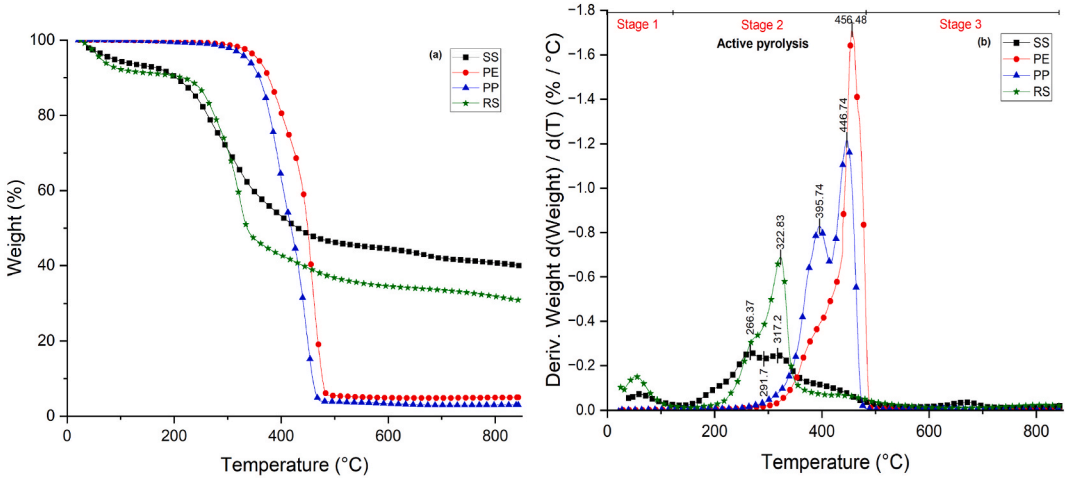

Fig. 3. (a) TG and (b) DTG curves of SS, PE, PP, and RS individual samples.

weight loss have been increased remarkably as starting from 350 °C, then their weight losses have been ended sharply at ~500 °C. While a sharp peak with a shoulder was observed in the pyrolysis profile of PE, PP has shown two separate sharp peaks in between 300 °C and 500 °C. This suggests that there may be some additives in PP composite label wastes as coming from laminates, coatings, fillers etc.

For the third decomposition stage, since lignin is more complex than that of hemicellulose or cellulose, it decomposes in a wide temperature range in between 300 and 600 °C by partly overlapping with cellulose and hemicellulose degradation profiles. As it can be seen from the DTG curves in Fig. 3(b), a broad peak in this region was remarkable for RS and was given to its lignin content. A similar weight loss trend in this region was noticed for SS as well. However, the part of this broad peak until 500 °C for SS was overlapping with the profile of plastic decomposition and can be attributed to the decomposition of micro-plastics as well. Lastly, minor mass losses were recorded in the temperatures >600 °C. A small but distinct peak was particularly notable for sewage sludge. The weight losses in this high temperature region can be attributed to the decomposition of non-biodegradable organics and inorganics such as carbonates ($CaCO_3$) and microclines, particularly present in SS [37,38]. Finally, the weight loss has reached a stable plateau near zero until 850 °C. Similar trends and observations have been reported by some other authors as well [15,20,39–42].

The decomposition rates for these three feedstocks have been calculated for the second stage of decomposition where the main pyrolysis reactions occur in between 200 and 500 °C. The calculated decomposition rates for sewage sludge were 1.15 mg/s at 275 °C and 1.05 mg/s at 325 °C. In the other side, rice straw has displayed a significant increase in decomposition rates particularly at 325 °C as being of 2.6 mg/s without a marked shift in peak temperatures. All these can be ascribed to their similar cellulosic constituents but with the higher amounts in case of the rice straw. Plastics with totally different chemical nature have exhibited a significant shift in decomposition peak temperatures together with the concurrent increase in the decomposition rates. The highest decomposition rate of 9.0 mg/s at 456 °C was recorded for polyethylene whereas the decomposition rate at 446 °C was 6.29 mg/s for polypropylene. The highest decomposition rates of plastics can be assigned to high volatile content. However, the lower decomposition peak temperatures in case of sewage sludge and rice straw may be from improved kinetics.

As seen in Fig. 3(b), the observed degradation rates have followed the order of PE > PP > RS > SS and the maximum weight loss rate was observed at 455 °C for PE, followed by at 445 °C for PP, at 310 °C for RS and at 255 °C for SS. As seen in Fig. 3(a), PP had the highest total weight loss of 97 wt%, followed by 95 wt% for PE, 69 wt% for RS and 60 wt% for SS. The measured char yields were 39.99 %, 30.92 %, 4.97 % and 2.98 % for SS, RS, PE and PP, respectively. The reason for the higher residue amount of SS compared to the other feedstock was that SS has a higher ash content of 39.4 %. All these results were in agreement with the proximate analysis results.

3.2.2. *Thermogravimetric analysis of SS, PE and PP blends*

The thermogravimetric decomposition profiles under pyrolysis condition for the blends of sewage sludge (SS) and plastic (PE and PP) were shown in Fig. 4(a and b). The calculated and measured char yields according to Equations (2) and (3) for theoretical and actual values have been given in Table 4 as well.

A similar pyrolysis profile to single components in three stages has been noticed from the TGA/DTG figures for blends. As explained for TGA/DTG behavior of single components, thermal decomposition starts with the dehydration and the decomposition of the hydrated and light molecular weight volatiles up to 200 °C. Thermal decomposition continues as with the active pyrolysis region of 200–600 °C where depolymerization of biodegradable materials such as lipids, polysaccharides, cellulose through the bond breaking reactions. The secondary degradation of the components with less reactivity and high molecular weight happens as well. Beyond 600 °C, the third zone mass loss appears for the decomposition of inorganic substances like calcium carbonate. Although blends exhibited the decomposition characteristics of its constituents, some noticeable peak shifts in the active zone were observed in the presence of plastics. The peak maxima of the polyethylene blends were shifted from 452 °C for individual polyethylene to 475 °C and 470 °C for its blends of 1:1 and 3:1, respectively. Similarly, the peak maxima of the polypropylene blends were shifted slightly from

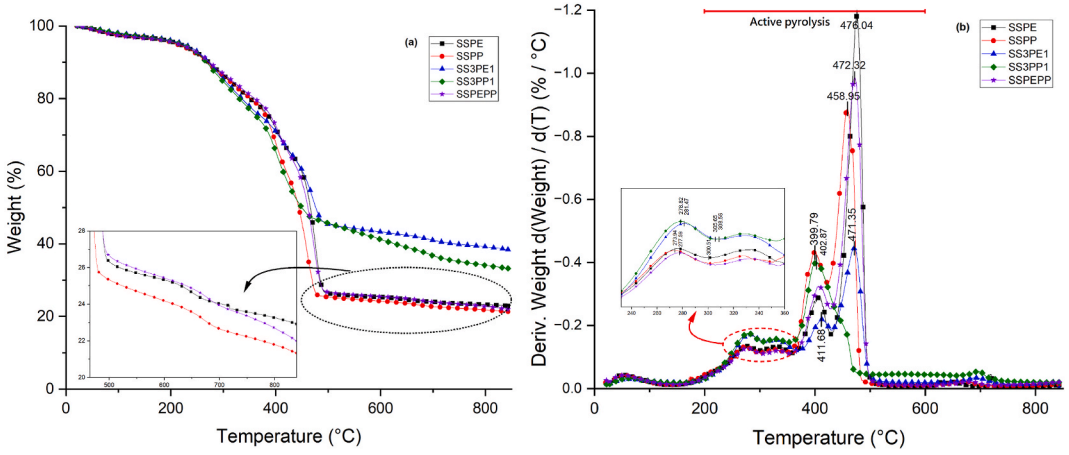

Fig. 4. (a) TG and (b) DTG curves of SS and plastics blends.

Table 4
The calculated and measured char yields for theoretical and actual values.

	SSPE	SSPP	SS3PE1	SS3PP1	SSPEPP
Actual Char Yield (%)	22.9	21.3	38.4	33.2	21.9
Theor. Char Yield (%)	22.5	21.5	31.2	30.7	22.0

445 °C to 455 °C and 450 °C for its blends of 1:1 and 3:1, respectively. This shift in the characteristic peak maxima for polyethylene blends was more distinct. As was explained by Vo et al. [43], plastic blends might decompose more slowly as compared to plastic itself because of the poor heat conductivity inside the biochar pores of sewage sludge and rice straw during co-pyrolysis since it requires a higher activation energy.

As given in Tables 3 and it is clear that the high ash content of sewage sludge would give char rich in inorganics. Therefore, it is reasonable for sewage sludge giving char yield as high as 40 %. On the other side, the polyethylene and polypropylene used in the study were composite wastes coming from the paper industry and hence it would be reasonable to have some char yields of 3–5%. Theoretical char yields of blends based on the measured char yields of its each constituent have been compared with the actual char yields in Table 4. It was noticed that actual char yields have deviated from the theoretical, especially for the blends of 3:1. This effect was more clear for the polyethylene blend of SS3PE1. This result can be interpreted in terms of secondary charring. As widely agreed on, primary char-volatile interactions are inevitable due to the H- and O-radicals present in the volatiles and the O-containing functional groups of char [44]. Since the biomass and plastics are in quite different chemical nature, they would have a different char-volatiles interactions. Although the mechanism of the interaction is quite complex and still unresolved, there is a consensus on the role of biochar promoting both the cracking of polyolefin volatiles and polymerization reactions. In the other side, H-radicals from the plastic volatiles might contribute to the ring condensation for char changing its crystallinity, surface functionality and internal structure. All these during the co-pyrolysis might lead to high char yields than expected under certain circumstances as of blends of 3:1 [44].

3.2.3. Thermogravimetric analysis of SS, PE, PP and RS blends

The thermogravimetric plots of sewage sludge (SS), plastics (PE and PP) and rice straw (RS) blends at different ratios were given in Fig. 5 (a) and 5 (b). The theoretical and measured char yields have been given in Table 5.

The total weight loss profile for all blends were shown to represent the decomposition characteristics of its constituents. To summarize again, classifying the weight loss profile into three regions: (1) moisture release at ~ 100 °C (2) organic matter decomposition at 200–500 °C and (3) CO_2 release from inorganic carbonates beyond 500 °C. The major weight losses were recorded in between 200 °C and 500 °C [45]. The similar TGA profiles of SS and RS can be ascribed to the high biomass residue content of SS. The only distinct feature of SS TGA was noticed as the shoulder around 400–450 °C possibly due to its micro-plastic content. TGA profiles of SS, RS and plastics (PE or PP) were as expected. However, the peaks from the decomposition of PE and PP have been slightly shifted to high temperatures in similar to TGA results of SS with plastic blends. As given in above mentioned discussions, this might be due to the melting of plastics on the interior surface of SS char, i.e. biochar, and poor heat transfer inside might lead the decomposition lagged on [46,47].

As expected, the residual char content upon pyrolysis has decreased in the presence of waste plastics, e.g. from 42.6 wt% for SSRS to 30.9 wt% for SSPERS upon polyethylene addition. The maximum weight loss at ~321 °C was recorded for SSRS blend. Upon increasing the SS content as of SS3RS1, the intensity of this peak has decreased and a shoulder at 400–450 °C became remarkable. This was attributed to the heterogeneous nature of SS composed of micro-plastics, lipids, proteins in addition to its biomass residues [48]. As of blends with waste plastics, two news peaks have been raised in between 400 and 500 °C at the expense of the peak intensity at 321 °C. It was obvious that more volatiles have been formed by increasing the plastics content in the final mix.

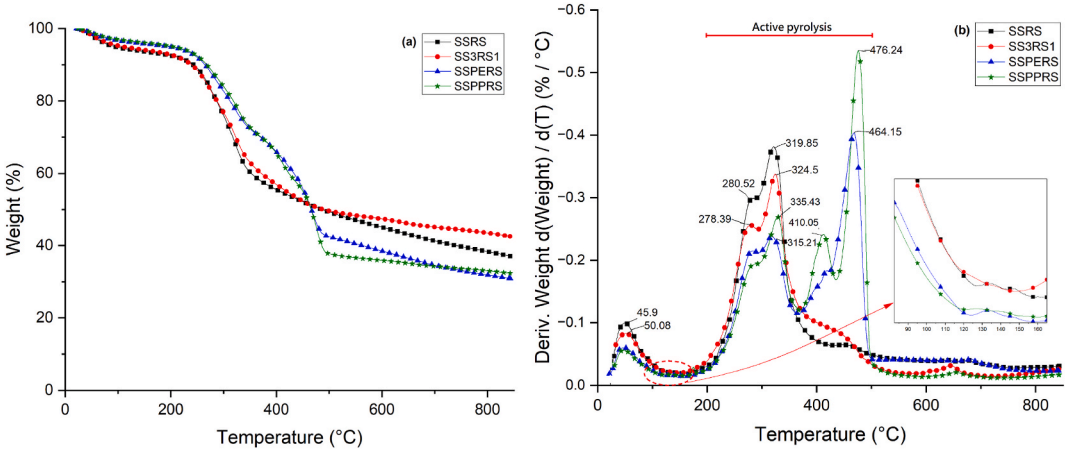

Fig. 5. (a) TG and (b) DTG curves of SS, RS, PE and PP blends.

Table 5
The calculated and measured char yields for theoretical and actual values.

	SSRS	SS3RS1	SSPERS	SSPPRS
Actual Char Yield (%)	37.1	42.6	30.9	32.3
Theoretical Char Yield (%)	35.5	37.7	28.9	30.8

As given in Table 5, the actual char yields of SS-RS blends were higher than the theoretical ones. In comparison to the SS-Plastics-RS blends, actual and theoretical values were varied more, i.e. actual and theoretical char yields of SS3RS1 blend were 42.6 % and 37.7 %, respectively. As argued before, the interaction mechanism between the two different feedstocks is quite complex and one can only speculate that H- and O-radicals generated by the early decomposition of biogenic wastes might have been interacted with the volatiles by micro plastics decomposition in sewage sludge that might be responsible for the secondary charring. All these findings have shown that a significant interaction or synergetic effect exists during the co-pyrolysis of SS, RS, PE and PP blends with a gradual increase in char yield.

3.3. Pyrolysis in rotary type batch pyrolysis unit

The pyrolysis experiments have been carried out at rotary type batch pyrolysis unit for sewage sludge. Operation conditions such as temperature and vapor residence time have been investigated to find out gas yield change with respect to liquid and char yields. In each of the experiments, the rotary bed reactor as operated at a fixed rotation speed of 5 Hz was charged with 0.5 kg of sewage sludge and the experiments were carried out at 750, 800 and 850 °C representing the high-temperature pyrolysis process. An inert atmosphere was maintained in the pyrolysis reactor by nitrogen flow of 0.5 L/min. This also ensured sweeping the condensable vapors out of the reactor. Char and oil have been collected from the reactor and downstream condensers and weighed for the overall mass balance calculations. The sum has been subtracted from the initial mass of biomass and was recorded as the gas yield. The calculated results have been corrected by omitting the ash content of the original feedstock in the overall mass balance. Therefore, yields were given on ash-free basis. The pyrolysis product distribution at three different temperatures has been given for sewage sludge (SS) in Fig. 6.

As seen in Fig. 6, gas yield has been continuously increased from 34.2 % to 40.0 % and then to 44.5 % with an increase in the pyrolysis temperature from 750 °C to 850 °C. The highest oil yield of 44.6 % was observed at the lowest temperature of 750 °C. The oil yield has decreased sharply to 37.0 % when the temperature was increased to 800 °C and then any further change in oil yield was not noticed at a further increase in temperature to 850 °C. In the other side, the char yield was fluctuated at around 20 %. It was shown that more facile decomposition of the macromolecular compounds in sewage sludge and their secondary cracking have resulted in the release of non-condensable volatiles at 800–850 °C [49–52] since it was known that both linear and branched hydrocarbons lost their stability with temperature. As a result of this, their C-C bonds were more likely to be cracked giving more volatiles [53]. Lastly, the lowest char yield at 850 °C could be associated with its further volatilization via thermal cracking [10].

In the second sets of experiments, the temperature and rotational speed of the reactor were set to 850 °C and 5 Hz and inert nitrogen gas flow was changed from 0.5 L/min to 1.0 L/min and 1.5 L/min. Since the higher nitrogen flow rate gives the less residence time of the organic vapors inside the pyrolysis reactor, it can be a measure of accelerating the secondary cracking reactions. The effect of

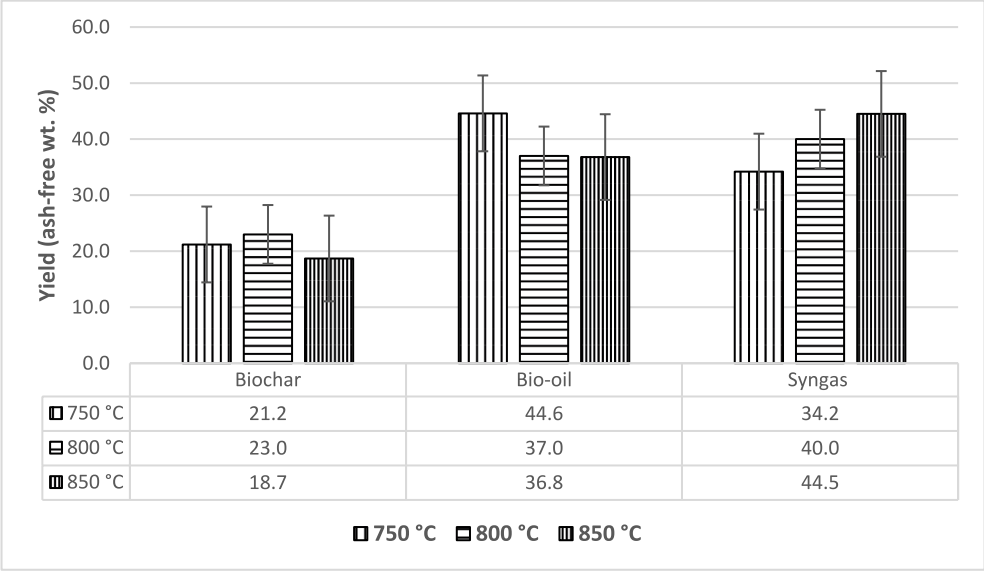

Fig. 6. Effect of different temperatures on SS pyrolysis products.

nitrogen flow rates on SS pyrolysis product distribution was shown in Fig. 7.

The effect of nitrogen flow was quite clear for 1.5 L/min as seen from Fig. 7. The highest liquid yield but the lowest gas yield of 55.5 % and 24.0 %, respectively, were obtained for the highest N_2 flow rate of 1.5 L/min, which is the minimum residence time condition. A slight increase in char yield was also noticed at increasing the flow rates as a measure of change in residence time. For the other nitrogen flow rates of 0.5 L/min and 1.0 L/min, these changes were not remarkable possibly due to insufficient flow turbulence inside the reactor without rigorous sweeping. Increasing the flow rates would permit the primary condensable vapors spend less time inside. This leads to less extended secondary cracking reactions giving a higher liquid but with a lower gas yield [54,55]. N_2 flow rate was set to 1.0 L/min to ensure complete inertness in subsequent experiments.

In the next phase, co-pyrolysis of sewage sludge (SS) with polyethylene, polypropylene and rice straw has been carried out at 850 °C and 1 L/min N_2 flow rate, favoring conditions for high gas yields. 1 L/min N_2 flow rate avoids blockage problems in case of plastic pyrolysis where wax formation had been observed in our previous experiments. The product yields during co-pyrolysis experiments in the batch reactor were presented in Fig. 8.

The main aim of the high temperature co-pyrolysis was to improve the gas yields and quality. The change in yields upon co-pyrolysis was due to the complicated interaction between the thermal decomposition intermediates. As it was widely accepted, thermal degradation is a radical chain reaction comprising radical initiation, chain propagation, and radical termination steps. Initially generated radicals from biomass and/or sewage sludge might promote the scission reactions for plastics giving more volatile products rather than wax. In the other side, plastics with a high H to C ratio might improve the pyrolysis oils via hydrogen transfer for its re-conditioning. This might end up with a decreased char yield as well [20,56].

As shown Fig. 8, the increase of PE and PP in the sewage sludge-plastic blends has led to an apparent increase in gas yields. Gas yields of 54.30 % and 60.38 % have been recorded at increasing the PE portion in the blend while it was 44.55 % for SS alone. Lower liquid yields of 25.46 % and 27.92 % were observed with increasing PE addition even that this decrease was not in proportion. Regarding the char yields, a remarkable decrease from 19.80 % to 11.70 % was for SS and SSPE, respectively but no significant change for SS3PE1. From the unreported experiments on plastics pyrolysis alone, one of the major products was wax rather than liquid. So, it was apparent that co-pyrolysis altered the degradation mechanism towards the formation of light volatiles and gaseous products. As explained above, the radical and hydrogen transfer mechanisms seemed effective in changing the product profiles to more gaseous products without wax formation. As for PE-SS blends, similar results have been observed for PP-SS blends. Increased gas yields at the expense of char and liquids was noticed clearly. Upon PP addition, gas yield has increased from 44.55 % to 62.03 % while char and liquid yields have been decreased from 19.80 % to 35.64 %–10.48 % and 27.50 %, respectively. In both cases, increased gas yields were not only the co-pyrolysis interactions but also originating from the much high volatile content of plastics. It was also likely that char gasification may be promoted during co-pyrolysis leading to an increase in gas yield.

In case of SS-RS blends, the results have some similarities as of SS-plastics. The higher volatile content of RS has contributed to the gas yield of SS-RS blends. Gas yields have increased from 44.55 % for SS to 45.14 % and 47.43 % for increasing RS content in their blends. The observed increases were not as pronounced as for plastic blends since the proximate analysis of SS and RS do not differ greatly each other. The volatile matter contents of SS and RS were 50.80 % and 60.62 %, and it was seen that this difference have been well reflected in the gas yield. The mechanism underlying the change of the product profile was believed to be still the same. Active radical intermediates might form during the cellulose pyrolysis, which is the main component of RS, through the thermal breakdown of oxygen-containing chemical bonds. As it was widely reported, cellulose undergoes a dehydrative inter-ring pathway at around 250 °C

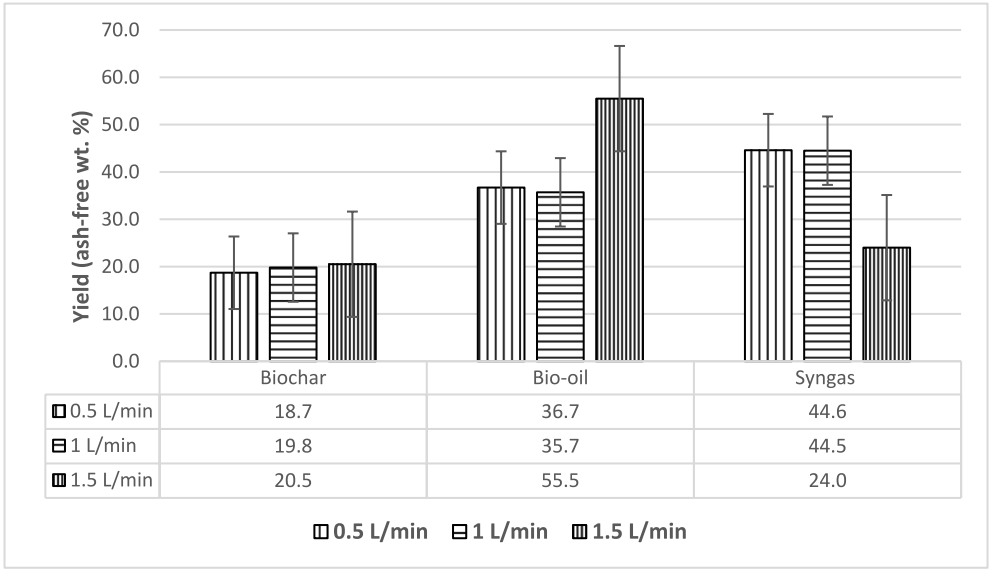

Fig. 7. Effect of different nitrogen flow rates on SS pyrolysis products.

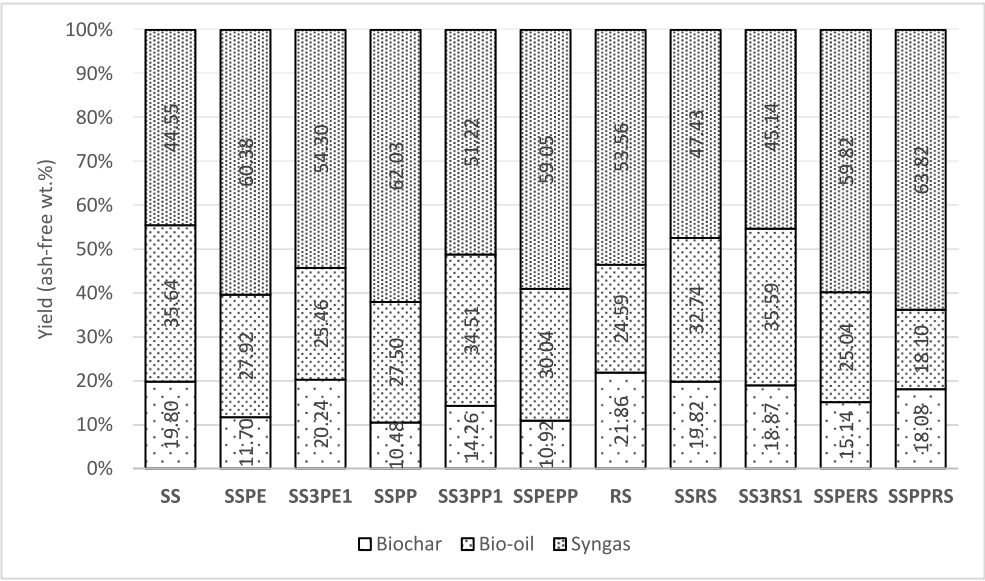

Fig. 8. Effect of co-pyrolysis of SS with PE, PP, and RS at different ratios on the product yields at 850 °C with a N_2 flow rate of 1 L/min.

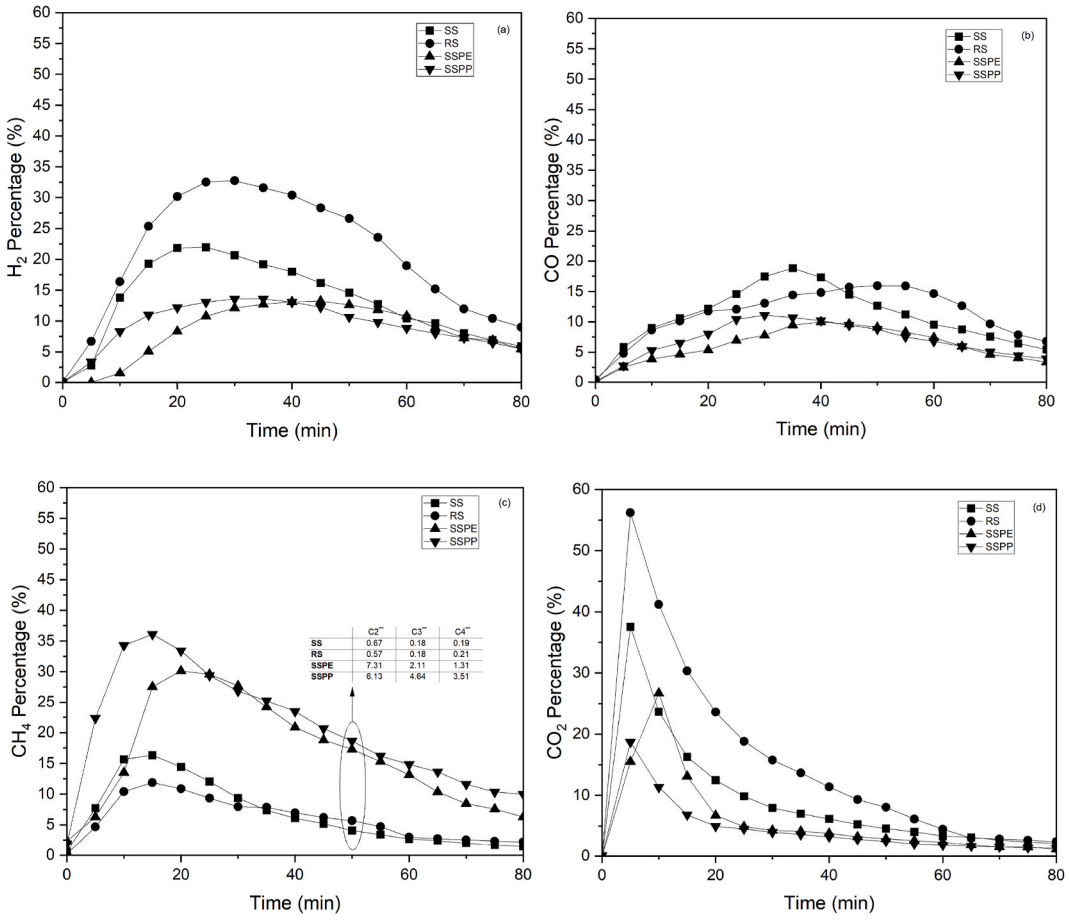

Fig. 9. (a) H_2, (b) CO, (c) CH_4 and (d) CO_2 gas percentage trends for SS, RS, SSPE, SSPP SSRS, SSPERS, SSPPRS and SSPEPP.

and loses its 10 % of weight as water. Upon increasing the temperature, its thermal degradation accelerated and charring might occur at sufficiently high temperatures [57]. In the other side, since sewage sludge contains not only cellulosic biomass residues but also micro-plastics, lipids and proteins, its pyrolysis products might differ during its co-pyrolysis with rice straw [58–60]. As cellulose has an early degradation temperature plateau, active radical intermediates are expected to be available to assist the sewage sludge pyrolysis and may help to change the sewage sludge degradation into more gaseous products.

For sewage sludge-rice straw-plastic blends, high gas yields were achieved. The gas yields around 60 % have been observed for the blends of SSPERS, SSPPRS as of SSPE and SSPP. In line with the binary mixtures, char and liquid yields were lower upon plastics and rice straw addition to sewage sludge. Char and liquid yields for SSPPRS were 18.08 % and 18.10 % while those for SSPERS were 15.14 % and 25.04 %. The results have clearly shown that gas yield increases with concomitant decrease in char and liquid yields for co-pyrolysis irrespective of the blend portions. The positive interaction might result from the appropriate ratio of SS, PE, PP, and RS. The inorganics in the ash content of sewage sludge and rice straw might also provide a catalytic effect on the secondary cracking reactions.

To wrap the studies up to this point, an optimum blending of SSPPRS exists when pyrolysis conditions were set to 850 °C under 1 L/min N_2 flow for the given reactor geometry. This validates the importance of the chemical characteristics of the feedstock such as ash content, fixed carbon, H/C and O/C ratios. All these were effective on the secondary cracking and reforming reactions towards gas yields increase. As of the target product, syngas yield was shown to be increased with the outstanding synergistic effects of co-pyrolysis. As a widely explained mechanism, gaseous products form through a series of reactions starting initially with the dehydration and decarboxylation reactions to give H_2O and CO_2. Then it proceeds with depolymerization and degradation to form condensable volatiles. Some of these volatiles are converted into syngas via secondary cracking and reforming reactions [3,61]. A6

ddition of plastics to sewage sludge can improve the gas yields due to its high volatile content. In the other side, ash content of sewage sludge might catalytically accelerate these secondary reactions. Moreover, intermediate radicals as formed through the early degradation of cellulose might facilitate the depolymerization/decomposition reactions of plastics. Lastly, hydrogen transfer from the plastics decomposition might have a stabilization effect on the initial degradation products of sewage sludge.

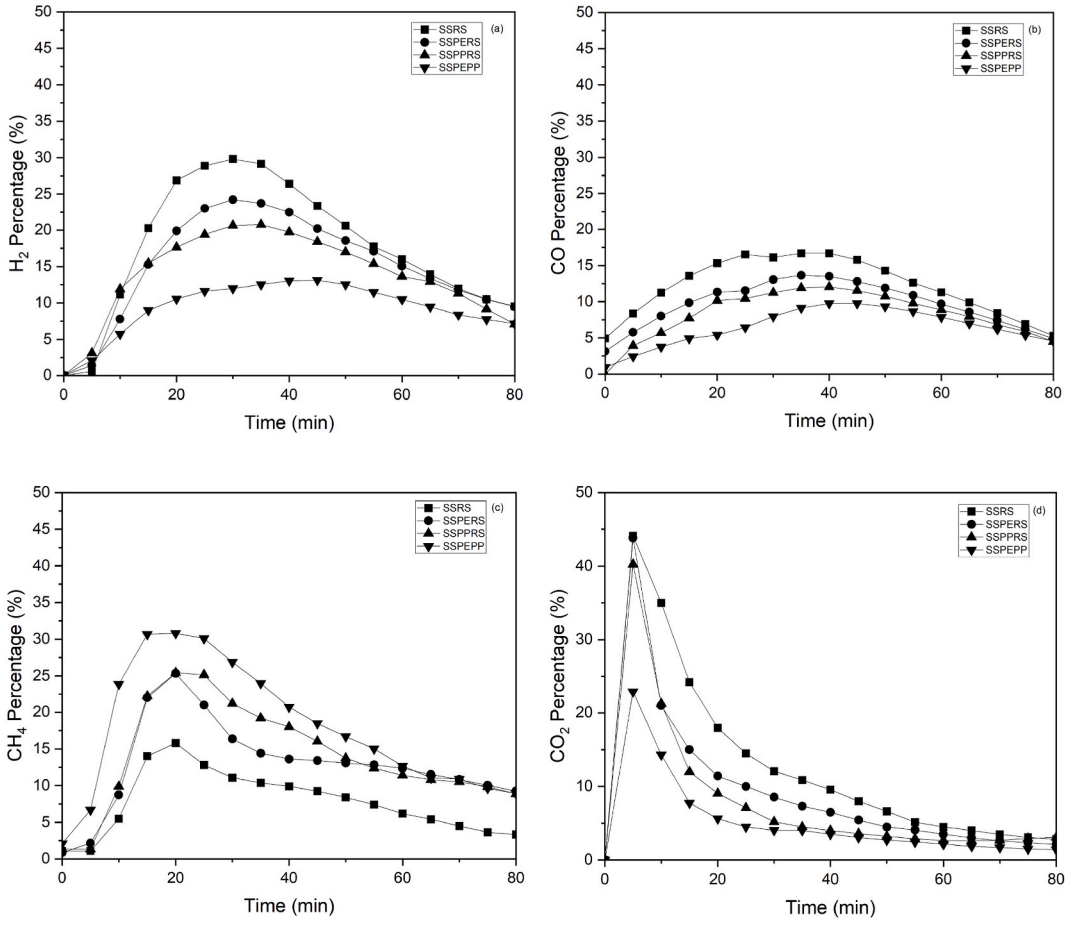

Fig. 10. (a) H_2, (b) CO, (c) CH_4 and (d) CO_2 gas percentage trends for SSRS, SSPERS, SSPPRS and SSPEPP.

3.4. Pyrolysis gas evolution trends in composition

The gas products of the pyrolysis experiments were monitored by on-line gas analyzer. The plots of gas compositions were given in Fig. 9 for sewage sludge, rice straw and sewage sludge-polyethylene or polypropylene mixtures in 50 % blending. Gas analysis results were nitrogen included without given in the plots.

As seen in Figs. 9 and 32.7 of % H_2 was achieved for the pyrolysis of rice straw. Those H_2 percentages for sewage sludge and its plastic blends were around 22 % and 13 %, respectively. Since sewage sludge contains both lignocellulose and micro-plastics fraction, hydrogen percentage by its pyrolysis was found to be higher than plastics but lower than rice straw, as in similar to CO_2 percentage and CH_4 percentage as well. The other marked difference between the gas evolution trends was the much higher initial CO_2 percentage for rice straw and sewage sludge. Initially, high CO_2 formation up to 60 % and 38 % was recorded for rice straw and sewage sludge, respectively. In the other side, much more methane formation was obvious upon plastic addition to the blend. CH_4 percentages were peaked to 30–35 % for either polyethylene or polypropylene containing blends. Lastly, broader CO percentage trends for all samples were clear. However, CO percentage on average was always higher for rice straw and sewage sludge than plastic containing blends. CO and CO_2 formations may initially arise due to the dehydration, decarbonylation (DCO) and decarboxylation (DCO_2) reactions all that remove oxygen in the form of water, carbon monoxide and carbon dioxide, respectively. CO/CO_2 is also generated through the reforming or cleavage of acetyl (CH_3CO–), ether (C–O–C) and/or ester (–COOR) bonds mostly exist in the biomass feedstock structure besides the secondary pyrolysis reactions for lignin [62,63]. By comparing the initial CO and CO_2 evolution trends, it appears that decarboxylation occurs before decarbonylation. This might be due to the exothermic nature of decarboxylation reactions favoring at low reaction temperatures. On the other hand, decarbonylation is slightly endothermic and continues to increase with temperature [63]. CO and CO % of the resultant pyrolysis gas mixture depends on the amount of carbonyl- and carboxyl-containing groups of the feedstock. Therefore, it was reasonable to have higher CO and CO_2 % in the gas product stream for oxygen rich feedstock such as rice straw and sewage sludge. Since the thermal stability of the feedstock is closely related to their chemical structures, they may have different pyrolysis gas evolution trends. Regarding methane, its formation from lignocellulose is related to the cracking of methoxyl (–O–CH_3), methyl (–CH_3), and methylene (–CH_2–) groups [62]. However, in case of plastic containing blends, methane formation mechanism changes to the random scission by the thermal degradation of the polymer as stated by Ref. [6]. The stabilization of the resultant radicals from the random scission process facilitates to carbon double bond formation leading to low molecular weight olefins such as ethene, propene, and butane [6,64]. This has been verified by the detection of light olefin species, seen as an inset the analysis results table in Fig. 9. Based on the analysis results on 50 min time on stream for sewage sludge, C_1, $C_{\overline{2}}$, $C_{\overline{3}}$ and $C_{\overline{4}}$ percentages were around 4.9 %, 0.7 %, 0.2 % and 0.2 %, respectively. With a rough approximation, those C_1, $C_{\overline{2}}$, $C_{\overline{3}}$ and $C_{\overline{4}}$ % values were seen to increase to around 15–20 %, 6–7%, 2–5% and 1–4% upon 50 % PE or PP plastic addition to sewage sludge. Comparing the polyethylene and polypropylene blends, an increase in propylene and butylene percentages have been noticed in case of PP blends. These have shown that pyrolysis of plastics or their blends are advantageous if the target products were methane or light olefins. In the other side, biomass origin feedstock would be the choice for syngas or hydrogen productions.

The pyrolysis gas compositions for the ternary mixtures of SSPERS, SSPPRS and SSPEPP were given in Fig. 10. For comparison, the SSRS binary mixture results were added as well. The highest H_2 % of 29.82 % was recorded for sewage sludge-rice straw blend (SSRS). With the addition of rice straw, the percentage of hydrogen has approached more closely to the percentage of H_2 achieved by pyrolysis of pure rice straw. This can be given to the rising synergistic effect as evidenced by the improved gas yields and H_2 formation during the co-pyrolysis of sewage sludge and rice straw blends. In the other side, maximum H_2 formation for sewage sludge-polypropylene/polypropylene-rice straw ternary blends were in the ranges of 20.7–24.4 %. This value was quite close to the value of 22 % that was measured during the pyrolysis of sewage sludge itself. That means plastic addition in ternary mixtures has ensured an improved

Table 6
The proximate and ultimate analysis results of chars from the batch pyrolysis tests.

Samples	PROXIMATE ANALYSIS (dry basis, wt. %)			ULTIMATE ANALYSIS (dry basis, wt. %)							
	Volatile	Ash	FC	C	H	N	S	O*	H/C	$\frac{(O+N)}{C}$	C/N
SSB-850	7.8	76.8	15.4	21.01	0.38	2.02	0.33	0.00	0.018	0.096	10.40
SSPEB	6.9	74.7	18.4	25.01	0.25	1.35	0.28	0.00	0.010	0.054	18.53
SS3PE1B	6.5	75.7	17.9	22.67	0.36	1.06	0.31	0.01	0.016	0.047	21.39
SSPPB	7.4	73.6	19.0	24.81	0.22	1.56	0.28	0.00	0.009	0.063	15.90
SS3PP1B	5.9	76.1	18.0	24.62	0.43	1.64	0.31	0.00	0.017	0.067	15.01
SSPEPPB	6.7	74.3	19.0	23.91	0.17	1.73	0.23	0.00	0.007	0.072	13.82
RSB	15.7	54.0	30.3	39.47	0.76	1.14	0.41	4.24	0.019	0.136	34.62
SSRSB	9.2	71.3	19.5	39.24	0.65	1.66	0.36	0.00	0.017	0.042	23.64
SS3RS1B	11.5	71.2	17.4	28.60	0.53	1.43	0.32	0.00	0.019	0.050	20.00
SSPERSB	10.3	70.8	18.9	33.00	0.59	1.61	0.22	0.00	0.018	0.049	20.50
SSPPRSB	10.5	70.5	19.0	31.07	0.55	1.58	0.27	0.00	0.018	0.051	19.66

SSB-X, biochar derived from SS single pyrolysis at 850 °C; RSB, biochar derived from RS single pyrolysis at 850 °C; SSPEB, SSPPB and SSRSB were blended biochars from co-pyrolysis SS with PE, PP and RS with 1:1 mixing ratio at 850 °C, respectively; SS3PE1B, SS3PP1B and SS3RS1B were blended biochars from co-pyrolysis SS with PE, PP and RS with 3:1 mixing ratio at 850 °C; SSPEPPB, SSPERSB and SSPPRSB were blended biochars from co-pyrolysis SS with PE and PP, SS with PE and RS and SS with PP and RS with 2:1:1 mixing ratio at 850 °C at 1 l/min of N_2 flow rate.
*By difference, O = 100–(C + H + N + S + Ash).

Table 7
Elemental composition of biochar samples detected by XRF.

Sample	Na_2O	MgO	Al_2O_3	SiO_2	P_2O_5	K_2O	CaO	TiO_2	Fe_2O_3	SO_3	Cl
	%	%	%	%	%	%	%	%	%	%	%
SS-850	0.36	2.24	11.93	34.89	8.62	3.07	6.57	0.93	4.64	0.77	0.09
SSPE	0.35	1.82	9.76	28.13	6.85	2.58	5.72	13.12	3.90	0.62	0.06
SSPP	0.41	1.96	11.50	30.95	7.54	2.80	6.19	3.88	4.21	0.68	0.06
SS3PP1	0.37	2.21	11.70	33.83	8.26	3.30	6.46	1.31	4.50	0.65	0.07
SSRS	1.21	1.82	6.26	33.96	4.61	4.15	4.41	0.55	3.01	0.67	1.60
SS3RS1	0.81	2.16	9.77	34.55	6.92	3.75	5.80	0.90	3.93	0.82	0.70
SSPPRS	0.88	1.84	7.83	32.81	5.36	3.67	4.88	1.21	3.44	0.70	0.93

gas yield as explained in section 3.3. but without sacrificing the H_2 formation. This can be regarded as the synergistic effect of plastic addition to biogenic wastes, namely rice straw, in terms of enhanced gas generation that is still rich in H_2. The lowest H_2 % of 13.0 % for the ternary mixtures of sewage sludge, polyethylene and polypropylene has supported the fact that the more the plastic content is the less the hydrogen % is due to the favoring C-C bond scission to methane. Similar trends have been observed for CO% and CO_2%. In line with this, an opposite situation has been clearly seen for methane selectivity values where methane formation has been steadily increased with an increase plastics share in the content of the ternary mixtures. When half of the ternary content was composed of polyethylene or polypropylene as of SSPEPP, the methane % was peaked up to 30.8 %, while if the plastics have been phased out from the content of the mixtures as in the case of SSRS, methane % was sharply dropped to 15.8 %. Therefore, it can be safely claimed here that gas yields can be improved for the ternary mixtures of sewage sludge, rice straw and plastics while keeping the hydrogen selectivity of the product gas as high as possible. This was partly explained by the synergistic effect among the biogenic wastes and plastics.

3.5. Biochar analysis

The proximate and ultimate analysis results of chars were shown in Table 6.

For all char samples, the volatile content as a measure of the progress of pyrolysis was reasonably much lower than the feedstock itself. For plastics with almost no fixed carbon and ash content, the char of sewage sludge-plastic blends has the similar characteristics of sewage sludge char as expected. As seen in Table 6, sewage sludge or its blends with plastics have volatile, ash and fixed carbon contents at around 6–8%, 73–76 % and 15–19 %. For rice straw and its blends, volatiles content of char was shown to be slightly more as compared to the chars from the pyrolysis of sewage sludge itself or its plastic blends. This situation can be reasoned by the pyrolysis progress be somewhat less in the presence of rice straw. Since rice straw has initially a fixed carbon content (11.6 %) as nearly doubled of sewage sludge feedstock (6.7 %), it was reasonable to have the highest fixed carbon (30.3 %) in its char.

To give insight on the synergistic effect during the co-pyrolysis of different feedstock, elemental analysis results have been evaluated. As widely accepted, the H/C molar ratio is a parameter that describes the carbonization degree and extent of char aromatization. A lower H/C ratio indicates a higher degree of carbonization [65]. Higher char stability is expected due to the increased aromatization making the bio-char less susceptible to oxidation in various environmental applications such as soil remediation [66]. This also might mean that more hydrogen would had been transferred into liquid and gas products. Lastly, the hydrophilicity and polarity of char are characterized by the O/C and (O + N)/C molar ratios, respectively [67]. A decrease in O/C and (O + N)/C molar ratios were also ascribed to the formation of more hydrophobic char with less polar surface groups. As seen in Table 7, H/C and (O + N)/C ratios were in general much lower for sewage sludge-plastic blends as compared to sewage sludge itself. For instance, while H/C and (O + N)/C ratios of sewage sludge were 0.018 and 0.096, SSPP char had those of 0.009 and 0.063, respectively. This might be possibly due to advanced char-volatiles interactions during co-pyrolysis. This interaction might alter the char yields and characteristics as well. In the other side, the high nitrogen content of sewage sludge dictates (O + N)/C ratio being high. In case of rice straw char, similar H/C of 0.019 but higher (O + N)/C was observed due to less oxygen content of sewage sludge feedstock. For all cases, nitrogen would partly be released in gaseous or tar forms as of HCN, NH_3 or organics.

3.5.1. Fourier transform-infra red spectroscopy (FTIR) analysis

The distribution of functional groups in the biochars was examined using FTIR. The FTIR spectra of the dried sewage sludge and chars produced under various pyrolysis and co-pyrolysis settings are shown in Fig. 11a and b.

As seen from the FT-IR of sewage sludge before pyrolysis, the small noisy peaks at around 693-796 cm^{-1} can be due to C-H bending groups of aromatic compounds. The major peak at 1002 cm^{-1} and with shoulders around it were ascribed to C=C bending of vinylidene groups and C–O stretching of polysaccharides or polysaccharide-like substances in sewage sludge. Amine groups have been noticed poorly at 1245 cm^{-1} due to C-N stretching. A broad peak around 1416-1438 cm^{-1} was given to the O-H bending of carboxylic acids. Two sharp bands at 1526 and 1640 cm^{-1} might be of protein origin amides. Aliphatic methylene groups have been identified by

the bands at 2925 and 2850 cm^{-1}. The broad band ranging in 3300–3500 cm^{-1} can be attributed to stretching vibration of bonded OH groups and water. Finally, two small bands appearing at 3700 cm^{-1} can be assigned to stretching vibrations of silanol groups as SiO–H [68]. Upon pyrolysis at 850 °C, the peaks assigned to surface amine, carboxylic acids and amides have been disappeared. However, the peaks in the band range of 700–1200 cm^{-1} still remain indicating the presence of inorganics such as carbonates, sulphates, phosphates and silica. Those small bands around 2360 cm^{-1} are from the carbon dioxide gas in the instrument rather than in the sample.

In case of sewage sludge-plastics blends, their FTIR profiles were quite similar to sewage sludge char at 850 °C. The only peak detected for these char samples were at around 700-1200 cm^{-1} showing the inorganic compounds as mentioned. However, the intensity of this peak decreases with increasing amount of plastics in blends since inorganics came from the sewage sludge itself. In the other side, the FTIR of sewage sludge-rice straw blends were nearly the same as of FTIR of sewage sludge. As it was observed for sewage sludge-plastic blends, the peak intensity coming from the inorganic content was less in comparison to sewage sludge. This is reasonable since sewage sludge contains more ash than rice straw.

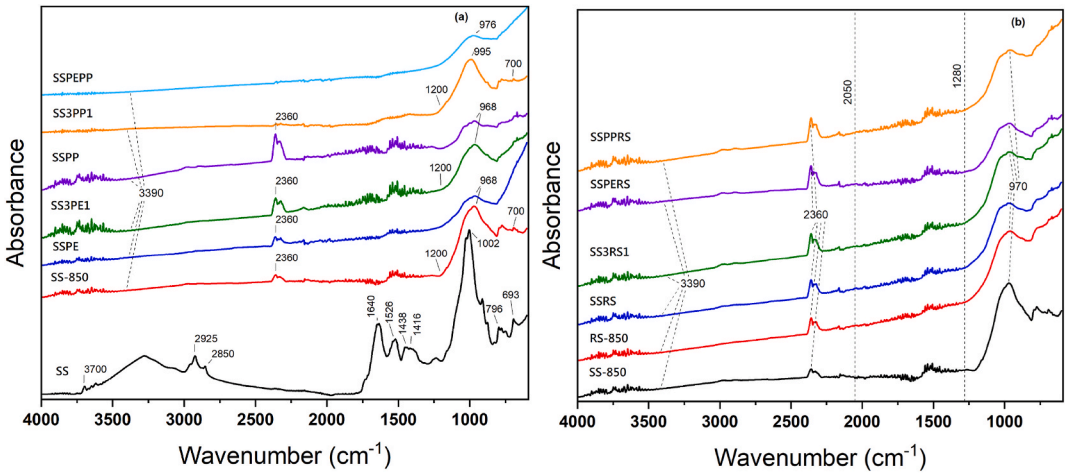

Fig. 11. FTIR spectra of the (a) raw material, SS biochar and biochar of SS and plastics blends; (c) SS and RS biochar and biochar of SS and RS blends.

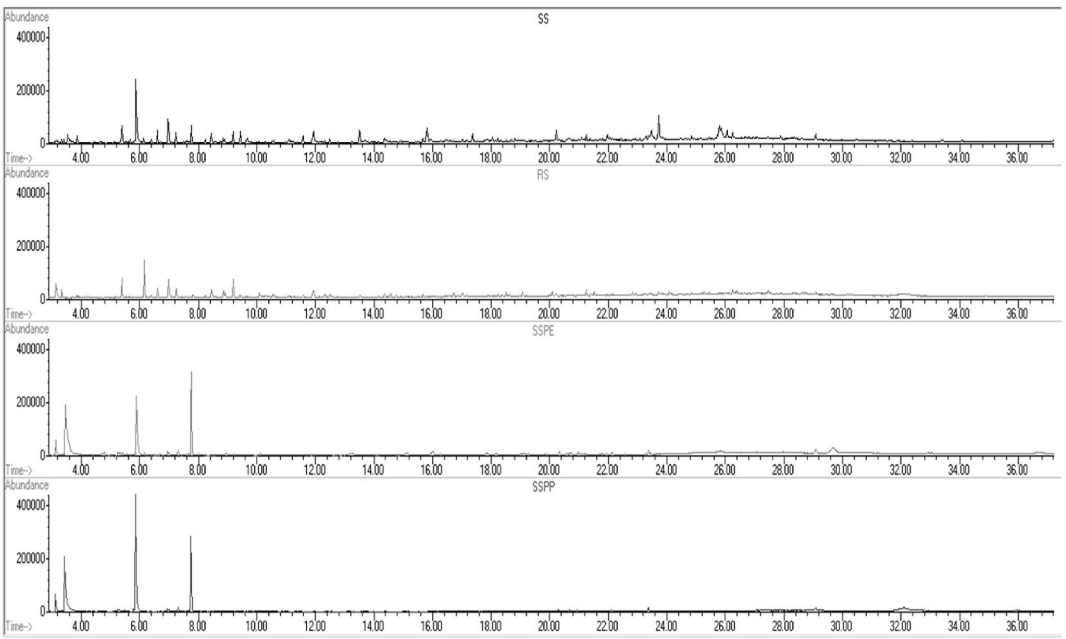

Fig. 12. The GC–MS chromatograms of bio–oil obtained from pyrolysis of SS, RS, SSPE and SSPP.

3.5.2. X-ray fluorescence (XRF) analysis

The distributions of elements of biochars obtained at different pyrolysis conditions were characterized using XRF analysis. XRF results for biochar samples were given in Table 7.

The inorganic compounds in high concentrations were SiO_2, Al_2O_3, P_2O_5 and CaO, respectively. It should be pointed out that TiO_2 concentration was much higher upon waste plastic addition to the blends since titanium dioxide was a typical filler used for packaging film manufacturing. Since rice straw was known as a straw with high ash and chlorine content, residual chlorine may exist in char after a significant release as water-soluble Cl and organic-bound chlorine. This has been reflected to XRF results of rice straw char. SS biochar has a high content of phosphorus close to 9 % as a potential for fertilizer. It was known that phosphorus is highly bioavailable for plants under non-oxidative conditions as pyrolysis as compared to oxidative conditions, i.e. incineration [69].

3.6. Bio-oil analysis

Bio-oil obtained from the pyrolysis of SS, RS and their blend with plastic wastes was subjected to GC-MS, and the spectrums obtained during GC-MS analysis are presented in Fig. 12.

Sewage sludge pyrolysis oil at 850 °C contains a mix of oxygenated compounds such as heterocyclic ketones, alcohols, diols, methoxy-phenolics, fatty acids and heterocyclic nitrogen-compounds such as cyclic imidic acids, alkyl amines, amides, indoles, triazoles, piperazines, triazines. Some of the identified major components by GC-MS were namely pentanone, furfuryl alcohol, cresol, furoic acid, pentenoic acid, palmitoleic & oleic acids, pyrrole, pyrrolidinone, piperidinone, 1,2-benzenediol and dimethoxyphenol.

Rice straw pyrolysis oil had a similar content with sewage sludge pyrolysis oil. However, some nitrogen compounds such as piperazines, piperidinone were missing possibly due to less nitrogen content of the feedstock. Moreover, fatty acids were not detected in rice straw based oil. The pyrolysis oil obtained with sewage sludge-rice straw blends had the characteristics of both depending on their mixing ratio.

In case of plastics and their blends with sewage sludge and rice straw, a more mud-like viscous oil was obtained. The fine fraction in the upper layer of this viscous oil was mainly composed of dimethyl heptane, alkyl cyclohexane, alkyl hexanol, indole, amino methyl or hydroxyl methyl pentanone, dimethyl piperazine, pyrrolidinone, tetra methyl piperidinone, methyl amino triazole, naphthalene, benzophenone etc. The waxy portion of the bottom oil would be expected to have high molecular weight aliphatic compounds rather than cyclic oxygenates [9,22,70,71].

3.7. Technical evaluation of the process by the bench vs pilot scale test results

Technical analysis of the process in terms of hydrogen production has been conducted on the results of the pyrolysis tests executed at both bench and pilot scales. Here, only one test at continuous pilot scale pyrolysis unit has been used to strength the importance of the batch scale pyrolysis research findings. However, a quite comprehensive continuing work on continuous pilot scale pyrolysis unit have recently been completed by the research team of this study. The research outcomes of this study will be shared in a continuing research paper where the mass and energy balance analysis on those data will be more meaningful in terms of commercial application practice. Therefore, an extensive mass and energy balance calculations have been intentionally left to the continuing research paper. In this respect, two specific tests executed on both batch and continuous units have been chosen on SSPPRS feedstock that was composed of 50 % sewage sludge, 25 % polypropylene and 25 % rice straw. The selection criterion for the pyrolysis of this feedstock was due to its highest gas yield of 63.8 % among all other feedstock pyrolysis test results recorded at the batch unit. The high gas yield for SSPPRS can be ascribed to its ideality for hydrogen production. The gas yield instead of H_2 % was consciously chosen as the selection parameter for hydrogen production since hydrogen concentration of the product gas can be increased in the downstream by the gas processing units such as water gas shift, steam methane reforming or catalytic cracking reactions.

With respect to batch unit pyrolysis test on SSPPRS, the gas analysis values reported here were the maximum values giving an idea of the reaction pathway. However, one should be aware of the fact that this was not sufficient for a thoroughly quantitative evaluation. On this basis, the highest H_2 percentage of 20.7 % was observed during the batch pyrolysis (Fig. 13) whereas the total of methane and C_2 to C_5 components was peaked up to 26.9 %. Methane content of it was 18 %. Besides, CO and CO_2 contents of pyrolysis gas at maximum were 12.4 % and 40.0 %, respectively.

In order to give an industrial insight on the hydrogen rich gas generation potential of SSPPRS, the same test at 850 °C has been carried out at pilot scale pyrolysis unit in continuous mode. The test on the same blend at continuous pilot scale unit were yield 75.06 % gas, 10.6 % oil and 14.34 % char on weight and ash free basis. For an understanding at a glance on the effect of the process mode, the gas composition trends of continuous pyrolysis unit with the top right inset of those of the batch unit were given in Fig. 13. The pyrolysis gas generated at pilot scale was composed of 35.33 % C_1–C_5, 32.35 % H_2, 20.26 % CO and 12.06 % CO_2 on average (balance N_2) and on volume basis. The H_2 and CO contents of pyrolysis gas have been increased as a result of an improved gas yield in continuous mode. Shortly, the marked differences when shifting from batch to continuous pyrolysis units were increased gas yields with syngas rich in H_2 and CO %. This is reasonable since different heat and mass transfer phenomena and fluid dynamics of these two pyrolysis units might lead a change in the pyrolysis chemistry. An elaborate analysis of these results has signed the fact that accelerated secondary reactions of volatiles were obvious in case of continuous pyrolysis. A long pyrolysis reactor integrated with hot cyclone had certainly played a role on an increased residence time and letting the condensable vapors spent more time in the hot zones. The secondary reactions of volatiles into non-condensable light gases might lead to combine the steam de-alkylation, reforming and cracking reactions to generate a H_2-rich gas. Water gas shift and Boudouard reactions might also had contributed to additional H_2 and CO. Since all these reactions proceeds secondarily, their occurrence should be favored by the increase of residence time and

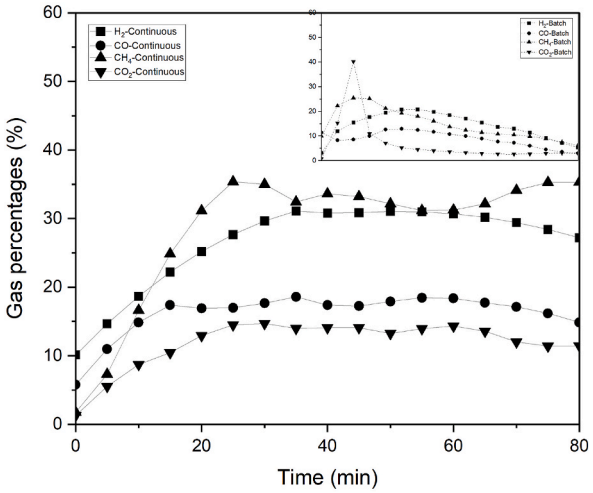

Fig. 13. Gas compositions trends for both batch and continuous pyrolysis tests on the feedstock consisting of 50 % sewage sludge, 25 % rice straw and 25 % waste polypropylene (abbreviated as SSRSPP).

temperature. As a result of this, hydrogen was seen as the main output of high temperature pyrolysis process with the occurrence of the following reactions:

$$C_nH_mO_k \rightarrow C_xH_yO_z + CO + CO_2 + CH_4 + C_nH_m + C$$

$$C_xH_yO_z + H_2O \rightarrow H_2 + CO + CO_2 + CH_4 + C_xH_y$$

$$CH_4 + CO_2 \leftrightarrow 2CO + 2H_2$$

$$CH_4 + H_2O \leftrightarrow CO + 3H_2$$

$$CO + H_2O \leftrightarrow CO_2 + H_2$$

$$2CO \leftrightarrow CO_2 + C$$

The high temperature pyrolysis provides several advantages over steam gasification and steam reforming of pyrolysis oil in the downstream. First, it combines the reactors in the same unit operating under optimum conditions. Secondly, high molecular weight tar formation and its load is suppressed, and finally high H_2 productions above 30 % can be attained. This hydrogen production can be further improved when the downstream operations have been configured accordingly. With a fully integrated waste to hydrogen solution, additional hydrogen can come up with the conversion of CO, CH_4, C_2-C_5 compounds into H_2 and CO_2 by applying the emerging tri-reformer concepts.

Waste to hydrogen are emerging as economically viable and environmentally sustainable solutions. From an economic standpoint, the potential benefits of waste to hydrogen comes from bringing the waste streams to economy by generating additional revenues. Pyrolysis can be applied to a variety of organic waste materials such as biomass, landfill waste, and organic industrial waste. Converting these waste streams into hydrogen helps to circular economy by lowering the disposal costs while also offering a renewable resource for hydrogen generation. Wastes are commonly offered at negative costs because they would otherwise necessitate costly disposal routes. Its low or negative cost availability makes waste to hydrogen process be a more economically viable solution. The waste to hydrogen production costs are estimated as of 1.5–4 € per kg of hydrogen which puts it in a very advantageous position relative to electrolyzers powered renewable hydrogen costs changing from €2 to €7 per kg. The multiple revenue opportunities make the pyrolysis route for waste to hydrogen be more attractive. First, the hydrogen is a valuable commodity both for energy and chemical sectors. Secondly, the by-products such as bio-char, vitrified slag, recovered phosphorous or siliceous components and pure carbon dioxide can find a market. Lastly, the excess thermal energy generated by the waste disposal process may also be used to meet heating demands. Additionally, As an economically attractive and environmentally benign waste disposal route, waste to hydrogen technologies strengthens the regional waste management systems by reducing their dependency on imported energy sources to foster the local economic development [72,73].

4. Conclusion

The highest decomposition rates of plastics can be assigned to high volatile content. However, the lower decomposition peak temperatures in the case of sewage sludge and rice straw may be from improved kinetics. In co-pyrolysis, the poor heat conductivity of biochar may retard the decomposition of plastics located in the pores. Char-volatile interactions were obvious from char yields increasing during co-pyrolysis. H- and O-radicals generated by the early decomposition of biomass to react with the volatiles by the plastics decomposition were agreed to be responsible for the secondary charring. Secondary reactions of volatiles favoring the gas yields were accelerated due to the increased residence time of condensable vapors. A combination of the secondary reactions, such as steam de-alkylation, reforming and cracking may be responsible for the conversion of condensable pyrolysis vapors into light gas fragments such as H_2, CO and CH_4. The synergistic effect of co-pyrolysis can be claimed to happen via the promoted random scission reaction on plastics assisted by the radicals generated from biogenic feedstock decomposition reactions. It was shown that high temperature pyrolysis has provided several advantages, such as high yield syngas generation, suppressed tar formation, facilitated downstream gas processing rather than complicated oil upgrading, and process intensification. This study has supported the fact that high temperature pyrolysis can be regarded as an emerging, economically competitive and environmentally sustainable solution for H_2 and biochar productions.

CRediT authorship contribution statement

Elif Babayiğit: Writing – review & editing, Writing – original draft, Visualization, Validation, Resources, Project administration, Methodology, Investigation, Funding acquisition, Formal analysis, Data curation, Conceptualization. **Dilek Alper:** Resources, Methodology, Investigation, Data curation. **Emine Çokgör:** Writing – review & editing, Writing – original draft, Validation, Supervision, Resources, Project administration, Methodology, Investigation, Funding acquisition, Formal analysis, Data curation, Conceptualization. **Hasan Can Okutan:** Writing – review & editing, Writing – original draft, Validation, Resources, Project administration, Methodology, Investigation, Funding acquisition, Formal analysis, Data curation, Conceptualization. **Alper Sarıoğlan:** Writing – review & editing, Writing – original draft, Validation, Supervision, Resources, Project administration, Methodology, Investigation, Funding acquisition, Formal analysis, Data curation, Conceptualization.

Declaration of competing interest

The authors declare the following financial interests/personal relationships which may be considered as potential competing interests:Prof.Dr. Hasan Can Okutan reports financial support was provided by Presidency of Strategy and Budget of the Presidency of Republic of Türkiye. If there are other authors, they declare that they have no known competing financial interests or personal relationships that could have appeared to influence the work reported in this paper.

Acknowledgments

This research was supported by the Scientific Research Projects of Istanbul Technical University (ITU BAP/Project No. 43396). Elif BABAYIGIT thanks Council of Higher Education (CoHE 100/2000 Ph.D. Scholarship Program) and TUBITAK (2211/A National Ph.D. Scholarship Program) for their support. The authors acknowledge greatly to Presidency of Strategy and Budget of the Presidency of Republic of Türkiye (Project No:2016K121250) for their funding on establishment of the research infrastructure that was used in this research as well.

References

[1] The Council of the European Communities, Council Directive of 12 June 1986 on the protection of the environment, and in particular of the soil, when sewage sludge is used in agriculture (86/278/EEC), Off. J. Eur. Communities - Legislation (1986) 5–6. https://eur-lex.europa.eu/legal-content/EN/TXT/PDF/?uri=CELEX:31986L0278.

[2] B. Zhao, X. Xu, H. Li, X. Chen, F. Zeng, Kinetics evaluation and thermal decomposition characteristics of co-pyrolysis of municipal sewage sludge and hazelnut shell, Bioresour. Technol. 247 (2018) 21–29, https://doi.org/10.1016/j.biortech.2017.09.008.

[3] J. Zhu, Y. Yang, L. Yang, Y. Zhu, High quality syngas produced from the co-pyrolysis of wet sewage sludge with sawdust, Int. J. Hydrogen Energy 43 (2018) 5463–5472, https://doi.org/10.1016/J.IJHYDENE.2018.01.171.

[4] S. Zhang, M. Pi, Y. Su, D. Xu, Y. Xiong, H. Zhang, Physiochemical properties and pyrolysis behavior evaluations of hydrochar from co-hydrothermal treatment of rice straw and sewage sludge, Biomass Bioenergy 140 (2020) 105664, https://doi.org/10.1016/j.biombioe.2020.105664.

[5] W. Li, J. Meng, Y. Zhang, G. Haider, T. Ge, H. Zhang, Y. Yu, S. Shan, Co-pyrolysis of sewage sludge and metal-free/metal-loaded polyvinyl chloride (PVC) microplastics improved biochar properties and reduced environmental risk of heavy metals, Environ. Pollut. 302 (2022) 119092, https://doi.org/10.1016/j.envpol.2022.119092.

[6] P.T. Williams, E.A. Williams, Interaction of plastics in mixed-plastics pyrolysis, Energy Fuel. 13 (1999) 188–196, https://doi.org/10.1021/ef980163x.

[7] Q. Chen, H. Liu, J.H. Ko, H. Wu, Q. Xu, Structure characteristics of bio-char generated from co-pyrolysis of wooden waste and wet municipal sewage sludge, Fuel Process. Technol. 183 (2019) 48–54, https://doi.org/10.1016/J.FUPROC.2018.11.005.

[8] Z. Wang, K. Liu, L. Xie, H. Zhu, S. Ji, X. Shu, Effects of residence time on characteristics of biochars prepared via co-pyrolysis of sewage sludge and cotton stalks, J. Anal. Appl. Pyrolysis 142 (2019) 104659, https://doi.org/10.1016/J.JAAP.2019.104659.

[9] Z. Ding, J. Liu, H. Chen, S. Huang, F. Evrendilek, Y. He, L. Zheng, Co-pyrolysis performances, synergistic mechanisms, and products of textile dyeing sludge and medical plastic wastes, Sci. Total Environ. 799 (2021) 149397, https://doi.org/10.1016/j.scitotenv.2021.149397.

[10] Y. Liu, Y. Song, J. Fu, W. Ao, A.A. Siyal, C. Zhou, C. Liu, M. Yu, Y. Zhang, J. Dai, X. Bi, Co-pyrolysis of sewage sludge and lignocellulosic biomass. Synergistic Effects on Products Characteristics and Kinetics, 2022, https://doi.org/10.1016/j.enconman.2022.116061.

[11] A. El-Naggar, S.S. Lee, J. Rinklebe, M. Farooq, H. Song, A.K. Sarmah, A.R. Zimmerman, M. Ahmad, S.M. Shaheen, Y.S. Ok, Biochar application to low fertility soils: a review of current status, and future prospects, Geoderma 337 (2019) 536–554, https://doi.org/10.1016/J.GEODERMA.2018.09.034.
[12] W. Zhang, C. Yuan, J. Xu, X. Yang, Beneficial synergetic effect on gas production during co-pyrolysis of sewage sludge and biomass in a vacuum reactor, Bioresour. Technol. 183 (2015) 255–258, https://doi.org/10.1016/J.BIORTECH.2015.01.113.
[13] H.S. Ding, H. Jiang, Self-heating co-pyrolysis of excessive activated sludge with waste biomass: energy balance and sludge reduction, Bioresour. Technol. 133 (2013) 16–22, https://doi.org/10.1016/J.BIORTECH.2013.01.090.
[14] X. Wang, S. Deng, H. Tan, A. Adeosun, M. Vujanović, F. Yang, N. Duić, Synergetic effect of sewage sludge and biomass co-pyrolysis: a combined study in thermogravimetric analyzer and a fixed bed reactor, Energy Convers. Manag. 118 (2016) 399–405, https://doi.org/10.1016/J.ENCONMAN.2016.04.014.
[15] S. Deng, H. Tan, X. Wang, F. Yang, R. Cao, Z. Wang, R. Ruan, Investigation on the fast co-pyrolysis of sewage sludge with biomass and the combustion reactivity of residual char, Bioresour. Technol. 239 (2017) 302–310, https://doi.org/10.1016/J.BIORTECH.2017.04.067.
[16] J.J. Klemeš, Y. Van Fan, R.R. Tan, P. Jiang, Minimising the present and future plastic waste, energy and environmental footprints related to COVID-19, Renew. Sustain. Energy Rev. 127 (2020) 109883, https://doi.org/10.1016/J.RSER.2020.109883.
[17] S. Bahl, J. Dolma, J.J. Singh, S. Sehgal, Biodegradation of plastics: a state of the art review, Mater. Today Proc. 39 (2021) 31–34, https://doi.org/10.1016/J.MATPR.2020.06.096.
[18] J. Shen, Y. Wu, G. Lan, Y. Xia, B. Yan, Y. Li, Y. Zhang, Y. Yu, C. Fu, A. Xu, J. Zhou, A. Zhu, D. Chen, Effect of co-pyrolysis of sewage sludge with different plastics on the nitrogen, sulfur, and chlorine releasing characteristics and the heavy metals ecological risk of biochar, J. Environ. Chem. Eng. 11 (2023) 110406, https://doi.org/10.1016/J.JECE.2023.110406.
[19] J. Chattopadhyay, T.S. Pathak, R. Srivastava, A.C. Singh, Catalytic co-pyrolysis of paper biomass and plastic mixtures (HDPE (high density polyethylene), PP (polypropylene) and PET (polyethylene terephthalate)) and product analysis, Energy 103 (2016) 513–521, https://doi.org/10.1016/J.ENERGY.2016.03.015.
[20] A. Zaker, Z. Chen, M. Zaheer-Uddin, J. Guo, Co-pyrolysis of sewage sludge and low-density polyethylene – a thermogravimetric study of thermo-kinetics and thermodynamic parameters, J. Environ. Chem. Eng. 9 (2021) 104554, https://doi.org/10.1016/J.JECE.2020.104554.
[21] X. Kai, R. Li, T. Yang, S. Shen, Q. Ji, T. Zhang, Study on the co-pyrolysis of rice straw and high density polyethylene blends using TG-FTIR-MS, Energy Convers. Manag. 146 (2017) 20–33, https://doi.org/10.1016/J.ENCONMAN.2017.05.026.
[22] X. Tang, X. Chen, Y. He, F. Evrendilek, Z. Chen, J. Liu, Co-pyrolytic performances, mechanisms, gases, oils, and chars of textile dyeing sludge and waste shared bike tires under varying conditions, Chem. Eng. J. 428 (2022) 1385–8947, https://doi.org/10.1016/j.cej.2021.131053.
[23] S.S.A. Syed-Hassan, Y. Wang, S. Hu, S. Su, J. Xiang, Thermochemical processing of sewage sludge to energy and fuel: fundamentals, challenges and considerations, Renew. Sustain. Energy Rev. 80 (2017) 888–913, https://doi.org/10.1016/j.rser.2017.05.262.
[24] Y.F. Huang, W.R. Chen, P.T. Chiueh, W.H. Kuan, S.L. Lo, Microwave torrefaction of rice straw and pennisetum, Bioresour. Technol. 123 (2012) 1–7, https://doi.org/10.1016/J.BIORTECH.2012.08.006.
[25] J.L. Shie, C.Y. Chang, C.S. Chen, D.G. Shaw, Y.H. Chen, W.H. Kuan, H.K. Ma, Energy life cycle assessment of rice straw bio-energy derived from potential gasification technologies, Bioresour. Technol. 102 (2011) 6735–6741, https://doi.org/10.1016/J.BIORTECH.2011.02.116.
[26] S. Dharmaraj, V. Ashokkumar, R. Pandiyan, H.S. Halimatul Munawaroh, K.W. Chew, W.H. Chen, C. Ngamcharussrivichai, Pyrolysis: an effective technique for degradation of COVID-19 medical wastes, Chemosphere 275 (2021) 130092, https://doi.org/10.1016/J.CHEMOSPHERE.2021.130092.
[27] T. Waldheim, L. Nilsson, Heating value of gases from biomass gasification. http://www.ieatask33.org/app/webroot/files/file/publications/HeatingValue.pdf, 2001. (Accessed 11 February 2024).
[28] L. Zhao, X. Cao, O. Mašek, A. Zimmerman, Heterogeneity of biochar properties as a function of feedstock sources and production temperatures, J. Hazard Mater. 256 (2013) 1–9, https://doi.org/10.1016/j.jhazmat.2013.04.015.
[29] N. Marin, S. Collura, V.I. Sharypov, N.G. Beregovtsova, S. V Baryshnikov, B.N. Kutnetzov, V. Cebolla, J. V Weber, Copyrolysis of wood biomass and synthetic polymers mixtures. Part II: characterisation of the liquid phases, J. Anal. Appl. Pyrolysis 65 (2002) 41–55. www.elsevier.com/locate/jaap. (Accessed 23 March 2024).
[30] Y. Zhang, C. Zhou, Z. Deng, X. Li, Y. Liu, J. Qu, X. Li, L. Wang, J. Dai, J. Fu, C. Zhang, M. Yu, H. Yu, Influence of corn straw on distribution and migration of nitrogen and heavy metals during microwave-assisted pyrolysis of municipal sewage sludge, Sci. Total Environ. 815 (2022) 152303, https://doi.org/10.1016/J.SCITOTENV.2021.152303.
[31] M.H.M. Ahmed, N. Batalha, H.M.D. Mahmudul, G. Perkins, M. Konarova, A review on advanced catalytic co-pyrolysis of biomass and hydrogen-rich feedstock: insights into synergistic effect, catalyst development and reaction mechanism, Bioresour. Technol. 310 (2020) 123457, https://doi.org/10.1016/J.BIORTECH.2020.123457.
[32] X. Hu, H. Guo, M. Gholizadeh, B. Sattari, Q. Liu, Pyrolysis of different wood species: impacts of C/H ratio in feedstock on distribution of pyrolysis products, Biomass Bioenergy 120 (2019) 28–39, https://doi.org/10.1016/J.BIOMBIOE.2018.10.021.
[33] C.C. Seah, C.H. Tan, N.A. Arifin, R.S.R.M. Hafriz, A. Salmiaton, S. Nomanbhay, A.H. Shamsuddin, Co-pyrolysis of biomass and plastic: circularity of wastes and comprehensive review of synergistic mechanism, Results in Engineering 17 (2023) 100989, https://doi.org/10.1016/J.RINENG.2023.100989.
[34] W.H. Chen, C. Naveen, P.K. Ghodke, A.K. Sharma, P. Bobde, Co-pyrolysis of lignocellulosic biomass with other carbonaceous materials: a review on advance technologies, synergistic effect, and future prospectus, Fuel 345 (2023) 128177, https://doi.org/10.1016/j.fuel.2023.128177.
[35] S.R. Naqvi, R. Tariq, Z. Hameed, I. Ali, S.A. Taqvi, M. Naqvi, M.B.K. Niazi, T. Noor, W. Farooq, Pyrolysis of high-ash sewage sludge: thermo-kinetic study using TGA and artificial neural networks, Fuel 233 (2018) 529–538, https://doi.org/10.1016/J.FUEL.2018.06.089.
[36] A. Zaker, Z. Chen, X. Wang, Q. Zhang, Microwave-assisted pyrolysis of sewage sludge: a review, Fuel Process. Technol. 187 (2019) 84–104, https://doi.org/10.1016/J.FUPROC.2018.12.011.
[37] Z. Chen, Q. Zhu, X. Wang, B. Xiao, S. Liu, Pyrolysis behaviors and kinetic studies on Eucalyptus residues using thermogravimetric analysis, Energy Convers. Manag. 105 (2015) 251–259, https://doi.org/10.1016/J.ENCONMAN.2015.07.077.
[38] M.B. Folgueras, M. Alonso, R.M. Díaz, Influence of sewage sludge treatment on pyrolysis and combustion of dry sludge, Energy 55 (2013) 426–435, https://doi.org/10.1016/J.ENERGY.2013.03.063.
[39] H. Jia, B. Liu, X. Zhang, J. Chen, W. Ren, Effects of ultrasonic treatment on the pyrolysis characteristics and kinetics of waste activated sludge, Environ. Res. 183 (2020) 109250, https://doi.org/10.1016/J.ENVRES.2020.109250.
[40] J. Yang, X. Xu, S. Liang, R. Guan, H. Li, Y. Chen, B. Liu, J. Song, W. Yu, K. Xiao, H. Hou, J. Hu, H. Yao, B. Xiao, Enhanced hydrogen production in catalytic pyrolysis of sewage sludge by red mud: thermogravimetric kinetic analysis and pyrolysis characteristics, Int. J. Hydrogen Energy 43 (2018) 7795–7807, https://doi.org/10.1016/J.IJHYDENE.2018.03.018.
[41] H. Xu, S. Cheng, D. Hungwe, K. Yoshikawa, F. Takahashi, Co-pyrolysis coupled with torrefaction enhances hydrocarbons production from rice straw and oil sludge: the effect of torrefaction on co-pyrolysis synergistic behaviors. https://doi.org/10.1016/j.apenergy.2022.120104, 2022.
[42] Q. Dong, S. Zhang, B. Wu, M. Pi, Y. Xiong, H. Zhang, Co-Pyrolysis of sewage sludge and rice straw: thermal behavior and char characteristic evaluations, Energy Fuel. 34 (2020) 607–615, https://doi.org/10.1021/acs.energyfuels.9b03800.
[43] T.A. Vo, Q.K. Tran, H.V. Ly, B. Kwon, H.T. Hwang, J. Kim, S.S. Kim, Co-pyrolysis of lignocellulosic biomass and plastics: a comprehensive study on pyrolysis kinetics and characteristics, J. Anal. Appl. Pyrolysis 163 (2022) 105464, https://doi.org/10.1016/J.JAAP.2022.105464.
[44] S.B. Engamba Esso, Q. Yan, Z. Xiong, X. Hu, J. Xu, L. Jiang, S. Su, S. Hu, Y. Wang, J. Xiang, Importance of char-volatiles interactions during co-pyrolysis of polypropylene and biomass components, J. Environ. Chem. Eng. 10 (2022) 108202, https://doi.org/10.1016/J.JECE.2022.108202.
[45] W.H. Chen, P.C. Kuo, A study on torrefaction of various biomass materials and its impact on lignocellulosic structure simulated by a thermogravimetry, Energy 35 (2010) 2580–2586, https://doi.org/10.1016/J.ENERGY.2010.02.054.
[46] A.O. Oyedun, C.Z. Tee, S. Hanson, C.W. Hui, Thermogravimetric analysis of the pyrolysis characteristics and kinetics of plastics and biomass blends, Fuel Process. Technol. 128 (2014) 471–481, https://doi.org/10.1016/J.FUPROC.2014.08.010.
[47] S. Xiong, J. Zhuo, H. Zhou, R. Pang, Q. Yao, Study on the co-pyrolysis of high density polyethylene and potato blends using thermogravimetric analyzer and tubular furnace, J. Anal. Appl. Pyrolysis 112 (2015) 66–73, https://doi.org/10.1016/J.JAAP.2015.02.020.

[48] S. Wang, G. Dai, H. Yang, Z. Luo, Lignocellulosic biomass pyrolysis mechanism: a state-of-the-art review, Prog. Energy Combust. Sci. 62 (2017) 33–86, https://doi.org/10.1016/J.PECS.2017.05.004.
[49] J. Jin, Y. Li, J. Zhang, S. Wu, Y. Cao, P. Liang, J. Zhang, M.H. Wong, M. Wang, S. Shan, P. Christie, Influence of pyrolysis temperature on properties and environmental safety of heavy metals in biochars derived from municipal sewage sludge, J. Hazard Mater. 320 (2016) 417–426, https://doi.org/10.1016/j.jhazmat.2016.08.050.
[50] C. Karaca, S. Sözen, D. Orhon, H. Okutan, High temperature pyrolysis of sewage sludge as a sustainable process for energy recovery, Waste Manag. 78 (2018) 217–226, https://doi.org/10.1016/j.wasman.2018.05.034.
[51] J. Oladejo, K. Shi, X. Luo, G. Yang, T. Wu, A review of sludge-to-energy recovery methods, Energies 12 (2019) 1–38, https://doi.org/10.3390/en12010060.
[52] Q. Xu, S. Tang, J. Wang, J.H. Ko, Pyrolysis kinetics of sewage sludge and its biochar characteristics, Process Saf. Environ. Protect. 115 (2018) 49–56, https://doi.org/10.1016/j.psep.2017.10.014.
[53] L. Wang, Y. Xu, Z. Zhao, D. Zhang, X. Lin, B. Ma, H. Zhang, Analysis of pyrolysis characteristics of oily sludge in different regions and environmental risk assessment of heavy metals in pyrolysis residue, ACS Omega 7 (2022) 26265–26274, https://doi.org/10.1021/acsomega.2c01994.
[54] S. Aramideh, Q. Xiong, S.C. Kong, R.C. Brown, Numerical simulation of biomass fast pyrolysis in an auger reactor, Fuel 156 (2015) 234–242, https://doi.org/10.1016/j.fuel.2015.04.038.
[55] Z. Boubacar Laougé, A.S. Çığgın, H. Merdun, Optimization and characterization of bio-oil from fast pyrolysis of Pearl Millet and Sida cordifolia L. by using response surface methodology, Fuel 274 (2020), https://doi.org/10.1016/j.fuel.2020.117842.
[56] P. Chen, Q. Xie, M. Addy, W. Zhou, Y. Liu, Y. Wang, Y. Cheng, K. Li, R. Ruan, Utilization of municipal solid and liquid wastes for bioenergy and bioproducts production, Bioresour. Technol. 215 (2016) 163–172, https://doi.org/10.1016/J.BIORTECH.2016.02.094.
[57] J. Scheirs, G. Camino, W. Tumiatti, Overview of water evolution during the thermal degradation of cellulose, Eur. Polym. J. 37 (2001) 933–942, https://doi.org/10.1016/S0014-3057(00)00211-1.
[58] J.N. Nigam, Ethanol production from wheat straw hemicellulose hydrolysate by Pichia stipitis, J. Biotechnol. 87 (2001) 17–27, https://doi.org/10.1016/S0168-1656(00)00385-0.
[59] J.G. Olsson, U. Jäglid, J.B.C. Pettersson, P. Hald, Alkali metal emission during pyrolysis of biomass, Energy Fuel. 11 (1997) 779–784, https://doi.org/10.1021/ef960096b.
[60] J. Werther, T. Ogada, Sewage sludge combustion, Prog. Energy Combust. Sci. 25 (1999) 55–116, https://doi.org/10.1016/S0360-1285(98)00020-3.
[61] X.Y. Lim, P.N.Y. Yek, R.K. Liew, M.C. Chiong, W.A. Wan Mahari, W. Peng, C.T. Chong, C.Y. Lin, M. Aghbashlo, M. Tabatabaei, S.S. Lam, Engineered biochar produced through microwave pyrolysis as a fuel additive in biodiesel combustion, Fuel 312 (2022) 122839, https://doi.org/10.1016/j.fuel.2021.122839.
[62] D. Chen, K. Cen, X. Zhuang, Z. Gan, J. Zhou, Y. Zhang, H. Zhang, Insight into biomass pyrolysis mechanism based on cellulose, hemicellulose, and lignin: evolution of volatiles and kinetics, elucidation of reaction pathways, and characterization of gas, biochar and bio-oil, Combust. Flame 242 (2022) 112142, https://doi.org/10.1016/j.combustflame.2022.112142.
[63] C. Liu, J. Huang, X. Huang, H. Li, Z. Zhang, Theoretical studies on formation mechanisms of CO and CO2 in cellulose pyrolysis, Comput Theor Chem 964 (2011) 207–212, https://doi.org/10.1016/J.COMPTC.2010.12.027.
[64] Y. Zhang, Z. Fu, W. Wang, G. Ji, M. Zhao, A. Li, Kinetics, product evolution, and mechanism for the pyrolysis of typical plastic waste, ACS Sustain Chem Eng 10 (2022) 91–103, https://doi.org/10.1021/acssuschemeng.1c04915.
[65] M.L. Cayuela, S. Jeffery, L. van Zwieten, The molar H:Corg ratio of biochar is a key factor in mitigating N2O emissions from soil, Agric. Ecosyst. Environ. 202 (2015) 135–138, https://doi.org/10.1016/j.agee.2014.12.015.
[66] J. Du, L. Zhang, T. Liu, R. Xiao, R. Li, D. Guo, L. Qiu, X. Yang, Z. Zhang, Thermal conversion of a promising phytoremediation plant (Symphytum officinale L.) into biochar: dynamic of potentially toxic elements and environmental acceptability assessment of the biochar, Bioresour. Technol. 274 (2019) 73–82, https://doi.org/10.1016/J.BIORTECH.2018.11.077.
[67] X. Zhu, Y. Liu, C. Zhou, G. Luo, S. Zhang, J. Chen, A novel porous carbon derived from hydrothermal carbon for efficient adsorption of tetracycline, Carbon N Y 77 (2014) 627–636, https://doi.org/10.1016/J.CARBON.2014.05.067.
[68] E. Smidt, P. Lechner, M. Schwanninger, G. Haberhauer, M.H. Gerzabek, Characterization of waste organic matter by FT-IR spectroscopy: application in waste science, Appl. Spectrosc. 56 (2002) 1170–1175, https://doi.org/10.1366/000370202760295412.
[69] M. Tomasi Morgano, H. Leibold, F. Richter, D. Stapf, H. Seifert, Screw pyrolysis technology for sewage sludge treatment, Waste Manag. 73 (2018) 487–495, https://doi.org/10.1016/J.WASMAN.2017.05.049.
[70] W. Chen, S. Shi, M. Chen, X. Zhou, Fast co-pyrolysis of waste newspaper with high-density polyethylene for high yields of alcohols and hydrocarbons, Waste Manag. 67 (2017) 155–162, https://doi.org/10.1016/J.WASMAN.2017.05.032.
[71] I. Uddin, G. Wang, D. Gao, Z. Hussain, M.Y. Naz, B. Hou, A. Hayat, Conventional and cement-catalyzed co-pyrolysis of rice straw and waste polyethylene into liquid and gaseous fuels by using a fixed bed reactor, Biomass Convers Biorefin (2021), https://doi.org/10.1007/s13399-021-01470-5.
[72] J. Lui, W.H. Chen, D.C.W. Tsang, S. You, A critical review on the principles, applications, and challenges of waste-to-hydrogen technologies, Renew. Sustain. Energy Rev. 134 (2020) 110365, https://doi.org/10.1016/j.rser.2020.110365.
[73] C. Warnes, A. Lesch, A Perspective on Scaling Low-Carbon Hydrogen Production, GREEN VS. BLUE HYDROGEN, 2022.